Drone-based Structure-from-Motion provides accurate forest canopy data to assess shading effects in river temperature models

Stephen J Dugdale[1,*,†], Iain A Malcolm[2], David M Hannah[1,*]

[1]School of Geography, Earth and Environmental Sciences, University of Birmingham, Edgbaston, Birmingham, B15 2TT

[2]Marine Scotland Science, Freshwater Fisheries Laboratory, Faskally, Pitlochry, PH16 5LB

*Correspondence to: stephen.dugdale@nottingham.ac.uk; d.m.hannah@bham.ac.uk

[†]Now at: School of Geography, University of Nottingham, University Park, Nottingham, NG7 2RD, UK

Full reference:

Dugdale, S.J., Malcolm, I.A., & Hannah, D.M. (2019). Drone-based Structure-from-Motion provides accurate forest canopy data to assess shading effects in river temperature models. *Science of The Total Environment*, 678, 326-340. DOI: 10.1016/j.scitotenv.2019.04.229

Accepted 15th April 2019; published online 8th May 2019

Abstract

Climatic warming will increase river temperature globally, with consequences for cold water-adapted organisms. In regions with low forest cover, elevated river temperature is often associated with a lack of bankside shading. Consequently, river managers have advocated riparian tree planting as a strategy to reduce temperature extremes. However, the effect of riparian shading on river temperature varies substantially between locations. Process-based models can elucidate the relative importance of woodland and other factors driving river temperature and thus improve understanding of spatial variability of the effect of shading, but characterising the spatial distribution and height of riparian tree cover necessary to parameterise these models remains a significant challenge. Here, we document a novel approach that combines Structure-from-Motion (SfM) photogrammetry acquired from a drone to characterise the riparian canopy with a process based temperature model (Heat Source) to simulate the effects of tree shading on river temperature. Our approach was applied in the Girnock Burn, a tributary of the Aberdeenshire Dee, Scotland. Results show that SfM approximates true canopy elevation with a good degree of accuracy (R^2 = 0.96) and reveals notable spatial heterogeneity in shading. When these data were incorporated into a process-based temperature model, it was possible to simulate river temperatures with a similarly-high level of accuracy (RMSE < 0.7 °C) to a model parameterised using 'conventional' LiDAR tree height data. We subsequently demonstrate the utility of our approach for quantifying the magnitude of shading effects on stream temperature by comparing simulated temperatures against another model from which all riparian woodland had been removed. Our findings highlight drone-based SfM as an effective tool for characterising riparian shading and improving river temperature models. This research provides valuable insights into the effects of riparian woodland on river temperature and the potential of bankside tree planting for climate change adaptation.

1. Introduction

There is increasing evidence that climate change will raise water temperatures in temperate- and high-latitude rivers (Garner et al. 2017a; Hardenbicker et al. 2017; Isaak and Rieman 2013). Many of the organisms that inhabit such water courses are cold water-adapted species (eg. salmonids) that are intolerant of high temperatures (Elliott and Elliott 2010; Jonsson and Jonsson 2009). It is therefore likely that climate change will alter the thermal suitability of these environments for fish and other aquatic fauna (eg. Hedger et al. 2013; Lynch et al. 2016; Poesch et al. 2016), potentially leading to geographical redistribution or structural changes in populations (eg. Comte et al. 2013; Myers et al. 2017; Ruiz-Navarro et al. 2016). In regions with reduced forest cover, elevated river temperatures in summer are often associated with a lack of bankside shading (eg. Detenbeck et al. 2016; Jackson et al. 2017; Johnson & Wilby, 2015). Consequently, riparian tree planting is increasingly advocated as a strategy for mitigating increasing river temperature extremes in summer (see Davies-Colley et al. 2009; Garner et al. 2017; Ghermandi et al. 2009; Guillozet 2015; Orr et al. 2015). However, while the processes by which riparian shading (and tree planting or clearcutting) modifies stream temperature are increasingly well-understood (eg. Dugdale et al. 2018; Garner et al. 2014; Gomi et al. 2006; Guenther et al. 2014; Guenther et al. 2012; Hannah et al. 2008; Leach and Moore 2017; Leach and Moore 2011; Roth et al. 2010; Sun et al. 2015), the effect of shading on temperature varies substantially between locations (eg. Brown & Krygier; 1970; Bowler et al. 2012; Holtby 1998; Moore et al. 2005a) with contrasting environmental characteristics. This means that the efficacy of riparian planting schemes can be highly variable between different rivers and regions. A better understanding of how and why the effects of riparian tree cover vary between rivers and regions is therefore central to informing optimal riparian tree planting strategies.

Process-based stream temperature models simulate the real-world mass and energy fluxes driving stream temperature dynamics (eg. Baker et al. 2018; Dugdale et al. 2017; Loinaz et al. 2013; Null et al. 2010; Yearsley, 2009) and consequently have the potential to elucidate the spatially and temporally variable effect of riparian tree cover on river temperature. These models often contain routines capable of simulating the impact of riparian shading on radiative (and to a lesser extent, turbulent) fluxes at the stream surface (eg. Chen et al.

1998a; LeBlanc et al. 1997; Rutherford et al. 1997; Sun et al. 2015). However, they are often difficult to parameterise, requiring extensive and detailed topographic data on catchment and channel characteristics and riparian tree heights in addition to spatio-temporally variable hydro-climatological data (eg. Chen et al. 1998b; Garner et al. 2017b; Justice et al. 2017; Trimmel et al. 2018; Fabris et al., 2018). While adequate data on catchment topography can usually be obtained using readily available mapping products and/or digital terrain models (DTMs), detailed information on riparian tree heights (which are often spatially heterogeneous and vary over time) can be challenging to obtain. This represents a key limitation for the use of process based models in remote regions or areas with highly variable forest cover.

There are several existing approaches for obtaining data on the spatial distribution and height of riparian vegetation. Hemispheric photography of the riparian canopy taken from the stream surface can be used to directly measure the amount of solar radiation blocked by bankside vegetation (Davies-Colley & Payne, 1998; Davies-Colley & Rutherford, 2005; Garner et al. 2014; Leach and Moore 2010; 2014; MacDonald et al. 2014; Moore et al. 2005b). While this approach produces arguably the highest-resolution representation of riparian shading, it is very field and laboratory intensive and so only practical over relatively short stream reaches. Consequently, many process-based stream temperature studies have used coarsely-spaced field observations (eg. vegetation elevation angles; Rutherford et al. 1997) or GIS polygons describing riparian buffer heights (Chen et al. 1998a; Fabris et al. 2018; Cox and Bolte 2007; Sridhar et al. 2004). With the exception of plantation agroforestry, these simplified approaches generally result in an imprecise representation of shading that reflects unrealistic spatial homogeneity in tree heights and locations (Loicq et al. 2018). More recently, a number of studies have demonstrated the utility of LiDAR-derived digital elevation data for accurately representing the impacts of bankside shading (Bachiller-Jareno et al. 2019; Justice et al. 2017; Loicq et al. 2018; Wawrzyniak et al. 2017). When incorporated in a process-based temperature model with appropriate shading routines, such data can help elucidate the stream temperature response to riparian shading over large distances (Loicq et al, 2018). However, despite these considerable advances, LiDAR data are a) often unavailable for remote/rural areas (eg. Scotland; see Scottish Government, 2012), b) can be costly to obtain and c) can be ill-suited for the characterisation of riparian shading as survey flights are often

conducted for other purposes (eg. flood risk assessment) and hence coincide with the leaf-off period (see Bachiller-Jareno et al. 2019).

Given these limitations, there is pressing need for alternative approaches that can provide detailed spatially heterogeneous information on tree locations and heights across intermediate spatial scales (1 – 10 km) for relatively low cost. Advances in image-derived topographic reconstruction using Structure-from-Motion (SfM) photogrammetry (see Fonstad et al. 2013; Westoby et al. 2012) mean that it is now possible to acquire high-accuracy, low-cost digital elevation data from small unoccupied aerial systems (sUAS; Carbonneau and Dietrich 2017). As a result, drone-based SfM has seen considerable interest in the river sciences for the derivation of a range of in-channel habitat metrics (eg. Dietrich 2017; Woodget and Austrums 2017). SfM has also been used to quantify riparian buffer vegetation (eg. Michez et al., 2016; 2017) and forest canopy height (eg. Birdal et al. 2017; Lisein et al. 2013; Wallace et al. 2016) with a high degree of accuracy. Indeed, the ability of SfM to generate high-resolution digital elevation data at relatively low cost suggests it could provide riparian tree height data of a similar quality to LiDAR but at a much reduced cost over smaller spatial scales. Such an approach would allow for the accurate characterisation of riparian shading in streams previously too small or remote to warrant LiDAR surveys, but difficult to cover with extensive field sampling such as hemispheric photography. This could substantially improve river temperature modelling in smaller sub-catchments of data-poor regions, where river temperatures can be highest and riparian shading most effective (Jackson et al., 2017). Furthermore, because of the low deployment costs of sUAS, it would be possible to acquire data during the optimal leaf-on period or at multiple time points to inform models relating to land management activities such as forest harvesting or tree planting. Despite showing considerable potential, the utility of SfM-derived riparian tree heights for computing shading effects on stream temperature has not yet been explored, thus its utility for generating accurate stream temperature predictions remains unknown.

This paper assesses the potential of a new methodology combining drone-based SfM and process-based river temperature modelling for characterising and understanding the effects of riparian woodland on the spatio-temporal variability of river temperature at intermediate spatial scales (10 – 10 km). We used SfM to measure

tree heights in a 2.2 km stretch of the Girnock Burn, an intensively studied tributary of the Aberdeenshire Dee, Scotland, and subsequently input these measurements into the Heat Source (Boyd and Kasper 2003) process-based stream temperature model to generate spatially and temporally variable water temperature predictions. Our specific objectives are to:

1. assess the ability of SfM to characterise spatial variability in riparian tree shading,
2. evaluate the accuracy of a stream temperature model parameterised using SfM tree height data,
3. compare stream temperature predicted using the SfM-parameterised model against the same model parameterised using LiDAR tree height data and
4. demonstrate the ability of this combination of SfM and process-based modelling to improve understanding of the effects of riparian shading on river temperature by comparing simulated temperatures to those from a model in which tree cover has been 'removed'.

2. Methods

2.1 Study area

The Girnock Burn drains the 30.3 km^2 catchment of Glen Girnock into the Aberdeenshire River Dee, a Special Area of Conservation (SAC) for Atlantic salmon that originates in the Cairngorm Mountains of the eastern Highlands of Scotland. The Girnock catchment ranges in height from 862 m to 230 m at the confluence with the River Dee (57.0515° N, 3.1048° W). Land use is predominantly heather moorland, although a mix of commercially planted conifer and semi-natural deciduous woodland is present within the lower 3.7 km of Girnock Burn where this study was focused. Low permability igneous and metamorphic bedrock overlain with glacial and glacio-fluvial sediments drive spatially variable groundwater inputs within the burn (Malcolm et al. 2005), although studies indicate that there are no major point-source groundwater contributions in the lower reaches that could substantially affect surface water temperature (Malcolm et al., 2005). The catchment receives ~1100 mm of annual precipitation (Tetzlaff et al. 2005b). Winter air temperatures generally remain between 0.5 - 4.0 °C while mean daily summer temperatures are generally between 11.0 - 13.5 °C (Langan et al. 2001; Hannah et al., 2004), although temperatures ranging from -27 to 31 °C have

previously been recorded in the catchment (Moir et al. 2002). Mean discharge measured at a Scottish Environmental Protection Agency (SEPA) gauging station (gauge ID 12004) located 1.3 km upstream from the confluence with the Dee is 0.52 m^3s^{-1}.

Our study focuses on a 2.2 km stretch situated immediately upstream of the confluence with the River Dee flowing in a north to north-east orientation (fig 1). The stretch is dominated by cobble and boulder morphology and has a mean bed width of ~8.0 m and a mean gradient of 0.016. The upstream limits of the study area marks a transition from open heather moorland terrain towards persistent bankside vegetation, which drives a substantial increase in the quantity of riparian shading. This increase in riparian shading has been shown to have a significant moderating effect on temperatures within the lower parts of Girnock Burn using a variety of physically and statistically based assessment approaches and qualitative description (Fabris et al. 2018; Garner et al. 2014, 2017; Imholt et al. 2013; Malcolm et al. 2008; Malcolm et al., 2004).

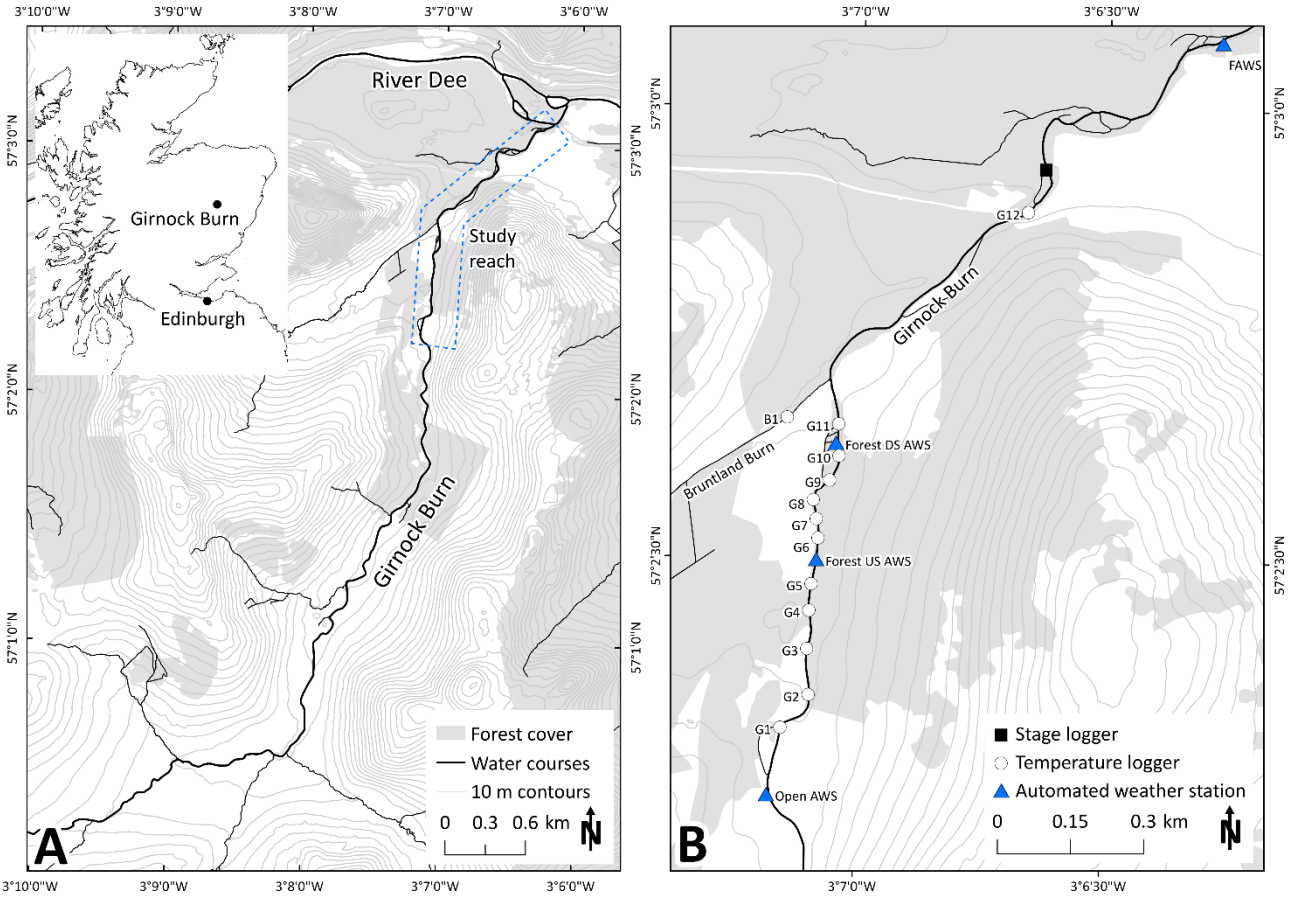

Figure 1. a) Girnock Burn with location of study reach marked (blue dashed polygon). b) Location of temperature loggers, automated weather stations and Marine Scotland gauging station within study reach

2.2 SfM data

2.2.1 Generation of SfM tree height raster

Aerial photography of a ~4 km by ~250 m strip covering the study stretch was acquired using a DJI Inspire 1 quadcopter equipped with a Zenmuse X3 gimbal-stabilised camera (4000 x 3000 px, standard RGB visible bands) in summer 2017. Owing to UK sUAS flight regulations which require drones to be flown within 500 m horizontal distance (and within line of sight) of the operator, the area was divided into five sub-sections which were each acquired separately. Following the recommendations of Carbonneau and Dietrich (2017) and James and Robson (2014), each sub-section was imaged from two separate altitudes (80 m and 100 m), with convergent imagery acquired at the higher of the two altitudes to minimise systematic error in the resulting SfM datasets. Flights were conducted over two days (14 and 17 July 2017); hydrometeorological conditions (river level, cloud cover) were relatively consistent between these periods. Ground control was provided by 61 ground control points (GCPs) distributed across the study stretch. The GCPs, consisting of 40 x 40 cm squares of blue tarpaulin pegged to the ground, were surveyed using a Leica Viva GS15 differential GPS running in RTK mode. Agisoft PhotoScan Professional (Agisoft 2017) was subsequently applied to the dataset (1660 images in total) to generate a ~10 cm resolution orthophoto (fig 2a) and digital surface model (DSM; fig 2b) of the area. Root mean square error (RMSE) of the SfM-derived DSM calculated against the GCPs was 0.11 m, 0.17 m and 0.10 m in the *x*-, *y*- and *z*-coordinates respectively. Following creation of the DSM, the SfM point cloud was classified using Agisoft PhotoScan's automatic ground point classification routine. The resulting 'ground only' point cloud was inspected and manually edited to ensure that points were correctly classified. A 10 cm 'bare earth' digital terrain model (DTM; fig 2c) was subsequently generated from the points corresponding to the (below-canopy) ground surface. Finally, a tree height raster of the study area was created by subtracting the DTM from the DSM (fig 2d).

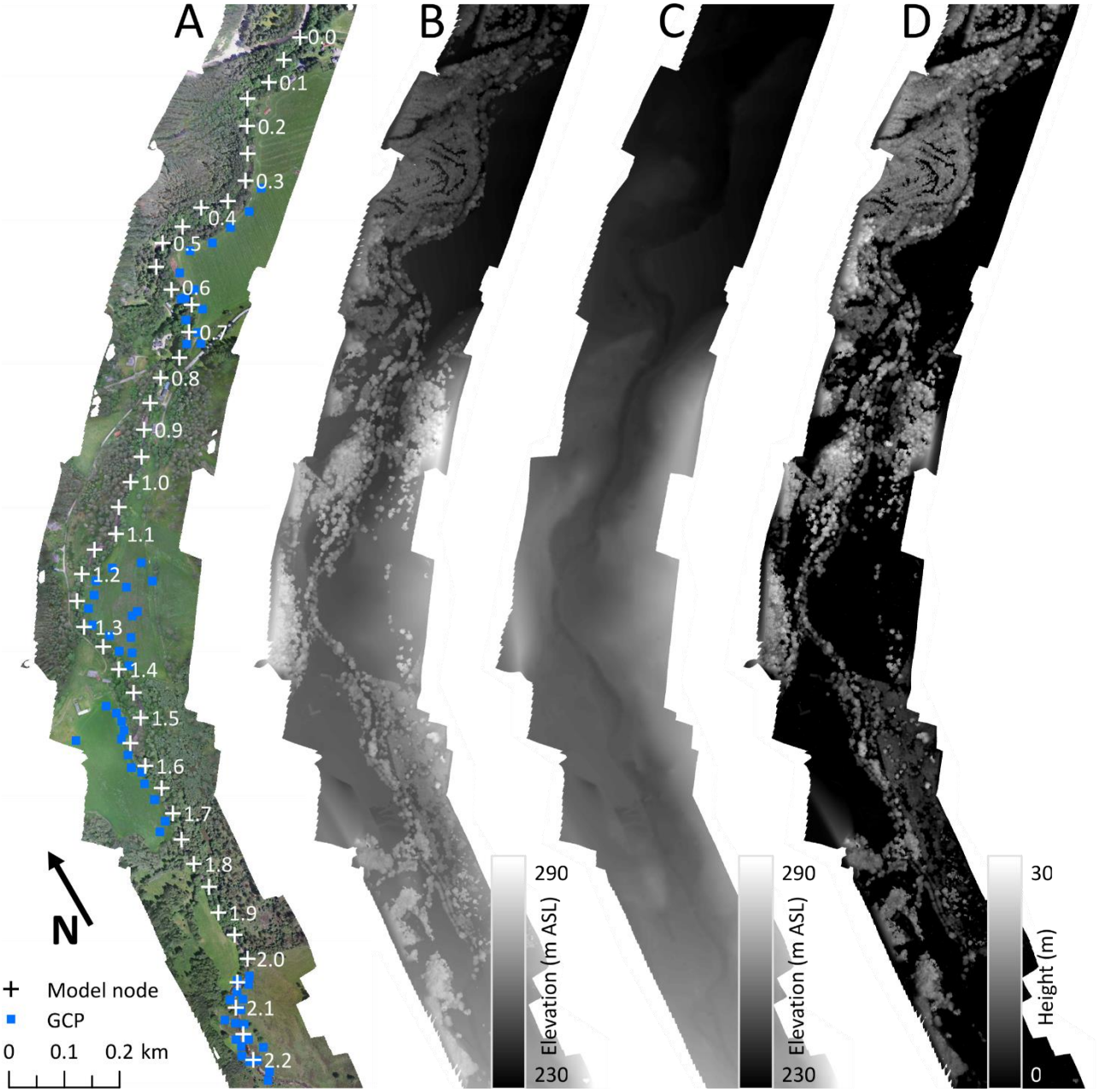

Figure 2. a) sUAS orthophoto of study reach with model nodes and ground control points (GCPs) marked. b) SfM-derived digital surface model (DSM) of study reach. c) Digital terrain model (DTM) created through from classification of SfM ground points. d) Tree height raster generated by subtracting DTM from DSM. Note north offset of -30°.

2.2.2 Assessing the accuracy of the SfM tree height raster

Although LiDAR data for the lower 1.7 km of the Girnock Burn exists as part of the *LiDAR for Scotland Phase I* dataset (Scottish Government, 2012), the large temporal and seasonal differences between the LiDAR dataset (leaf-off, acquired between March and May 2012) and the SfM survey (leaf-on, July 2018) meant that it was not appropriate to carry out a direct comparison of the SfM and LiDAR-derived tree height rasters due

to changes in leaf cover. Instead, we assessed the accuracy of the SfM-derived DSM and DTM separately, first by comparing canopy elevations in the SfM DSM to total station-derived observations acquired in the field, and then by comparing ground elevations in the SfM DTM to values derived from the LiDAR dataset.

To assess the extent to which the SfM-derived DSM approximated true riparian canopy elevation, we positioned a Leica Viva TS12 total station on a slope overlooking a ~800 m long (streamwise distance) section of the study stretch comprising variable tree cover (ie. a broad range of canopy elevations). Using the total station in reflectorless mode, we measured the elevations of the top of 63 tree crowns. Efforts were made to ensure that, despite some wind movement, measurements were taken as close to the top of the tree as possible. We subsequently extracted tree canopy elevations from the corresponding points in the SfM DSM. Comparison of the total station canopy elevations against those derived from the DSM indicates that SfM provides a good measure of 'true' canopy elevation (Fig 3A, $R^2 = 0.96$, RMSE = 1.16 m).

Because SfM is not able to penetrate the tree canopy as readily as other topographic reconstruction techniques (eg. LiDAR), it was also necessary to assess error in the 'bare earth' SfM digital terrain model, as any substantial error would propagate into the final tree height raster. The vertical accuracy of the resulting SfM DTM was therefore evaluated by comparing it to a LiDAR DTM of the lower 1.7 km of Glen Girnock derived from the *LiDAR for Scotland Phase I* dataset (Scottish Government, 2012). Cloud Compare (Cloud Compare 2018) was used to separate the LiDAR point cloud into tree canopy points (first returns) and ground points (last returns). The ground returns were densified (after Wawrzyniak et al., 2017) and rasterised to create a 1 m resolution LiDAR DTM. Elevations from the SfM and LiDAR DTMs were sampled using a mesh of gridded points at 10 m intervals located within a 100 m buffer of the stream channel. Only sections of the DTM that occurred under areas of tree canopy were sampled to avoid over favourable comparisons (as bare-ground elevations in areas absent of tree cover were extremely similar between the two datasets). Results of this comparison indicated that the SfM DTM was able to approximate the LiDAR bare ground elevations below the tree canopy with a high degree of accuracy (Fig 3B, $R^2 = 0.98$, RMSE = 1.25 m, bias = -0.35 m).

Given the logistical difficulty of field sampling tree heights over large areas and uncertainty in the 'real' treetop heights (owing to leaf cover and wind movement) a field measurement error on the order of ~1 m

might be expected. In light of the small differences between measured and modelled canopy elevations and good agreement between the ground points in the SfM and LiDAR DTMs, we determined that the SfM tree height raster was a good reflection of true tree heights in Girnock Burn.

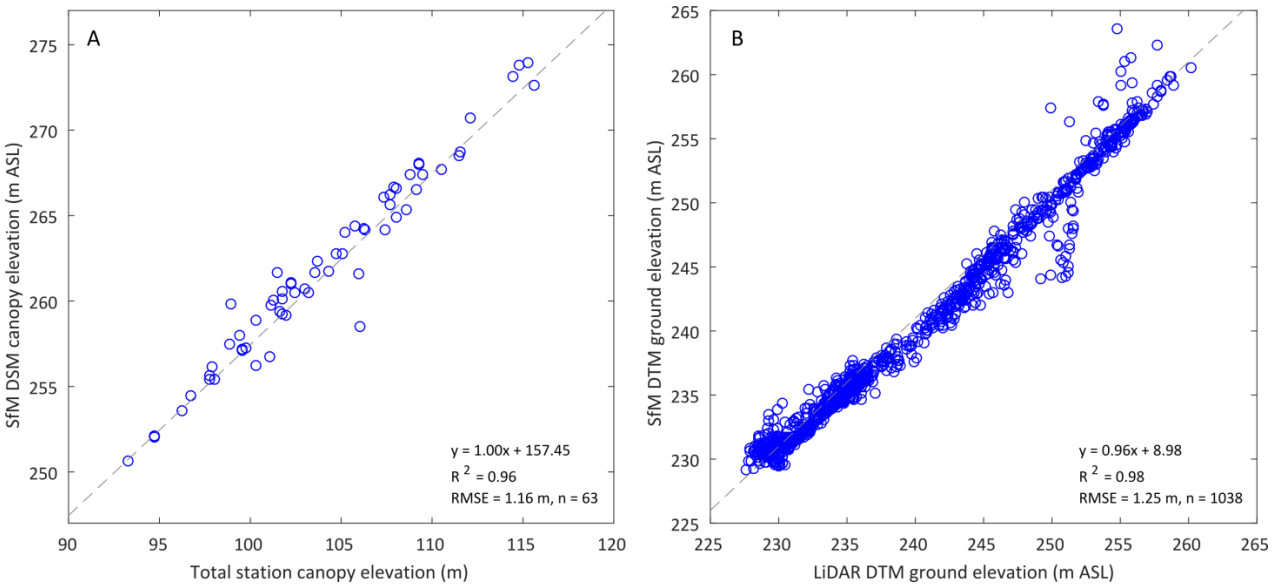

Figure 3. a) Comparison between SfM-derived tree canopy elevations (extracted from DSM) and total station observations (field measurements). b) Comparison between SfM and LiDAR-derived below-canopy elevations (extracted from DTM). Total station elevations are given relative to the total station (set at 100 m in the X,Y and Z coordinates), all other elevations are relative to mean sea level.

2.3 Temperature model

Stream temperature was modelled using Heat Source version 9.0.0b19 (available at https://github.com/rmichie/heatsource-9). An in-depth explanation of the model is beyond the scope of this article, although exhaustive details can be found in Boyd and Kasper (2003) and Trimmel et al. (2018). In brief, Heat Source is a process-based coupled hydraulic/river temperature model that simulates temperatures in a single (streamwise) dimension by calculating the net energy fluxes at each model node/timestep:

(1) $$H_{total} = H_{sw} + H_{lw} + H_e + H_s + H_b + H_a$$

where H_{total} represents the total energy gain (loss) by the river channel, H_{sw} is the net solar (shortwave) radiation flux, H_{lw} is the net longwave radiation flux, H_e is the latent heat flux, H_s is the sensible heat flux, H_b

represents heat conducted to or from the river bed and H_a is advective flux from tributaries, diffuse and local groundwater inputs and hyporheic exchange (all in W m^{-2}). The change in water temperature at each model node and timestep is computed as a function of energy gained or lost from the channel. Heat Source functions by simulating all of the above fluxes (with the exception of the tributary and groundwater components of H_a which are manually specified) using a series of physically-based and empirically-derived equations applied to input hydrometeorological and geomorphological data (see section 2.4). However, to improve model performance, we edited the *Python* source code to allow the use of direct observations of H_{sw} and H_b.

We chose to use Heat Source because it is one of the few readily available (ie. public and well-documented) process-based river temperature model that a) incorporates a detailed riparian shading model, b) can simulate stream hydraulics, c) allows for separate parameterisation of advective, groundwater (diffuse and localised) and hyporheic inputs and d) is easily customisable via modifications to its source code (see Dugdale et al., 2017 for a detailed review). Furthermore, Heat Source is specifically adapted to allow input of tree heights from raster geospatial data (such as SfM or LiDAR), and is thus ideally suited to this study. While we appreciate that Heat Source provides a slightly simplified representation of tree shading in comparison to some more comprehensive riparian shade routines (eg. DeWalle, 2008; 2011; Li et al. 2012; Rutherford et al. 2018a; 2018b), none of these models are readily available and/or permit the input of SfM/LiDAR data. Furthermore, the time required to develop a new model based on these principles was deemed prohibitive and inappropriate in a management context where the emphasis is often on the use of existing tools. Given that the purpose of our study is the demonstration of SfM as a potential source of tree height data for river temperature models, and in light of the fact that Heat Source is a well-established model in the literature (eg. Bond et al. 2015; Guzy et al. 2015; Justice et al. 2017; Kalny et al. 2017; White et al. 2017; Woltemade & Hawkins, 2016; Trimmel et al. 2018), it was deemed well-suited to this task.

2.3.1 Field data

Hydrometeorological, geomorphological and water temperature data for implementation/calibration of the Heat Source model were almost identical to those described by Garner et al. (2014). Meteorological data

were recorded by four automated weather stations (AWSs) deployed within the 2.2km study stretch (fig 1b) from October 2011 to July 2013. The upstream-most AWS was located outside of the forested riparian zone within an area of open moorland and thus recorded meteorological data uninfluenced by tree cover (Hannah et al., 2004); the remaining three AWSs were installed downstream of the transition from moorland to semi-natural forest cover under tree canopy cover. Each AWS measured air temperature (°C), relative humidity (%), wind speed (ms^{-1}), incoming shortwave (solar) radiation and bed heat flux (all Wm^{-2}) at 15 min intervals. Sensors for radiative and turbulent exchanges were installed at 2 m above the water surface under base flow, while the heat flux plate was buried at 5 cm depth in the stream bed; details on the specific instrumentation are the same as in Hannah et al. (2008). Heat Source requires measurements of cloud cover to compute H_{lw}; in the absence of direct observations, cloud cover was calculated using the equation:

(2) $$CC = \sqrt{1.54(1 - H_{sw,received}/H_{sw,potential})}$$ (Bond et al. 2015)

where $H_{sw,received}$ and $H_{sw,potential}$ are respectively the observed solar shortwave radiation (at the unshaded AWS) and the maximum solar shortwave radiation that would be possible under a cloudless sky (estimated from Heat Source's built-in solar radiation flux routines).

In terms of physiographic model input data, bed widths, channel gradient and near stream topography (for calculation of topographic/bank shading) were measured directly from the sUAS orthomosaic and DSM. River stage was recorded at a Marine Scotland Science (MSS) gauging station installed approximately 0.65 km upstream from the confluence with the River Dee (fig 1b); a stage discharge rating curve for the site (established using the velocity-area method; R^2 = 0.97) was used to generate a 15 min upstream boundary discharge series for Girnock Burn. An additional inflow discharge series for the Bruntland Burn tributary was calculated by scaling the discharge data by basin area. In the absence of observed discharge data for Bruntland Burn, we acknowledge that this scaling may influence temperature predictions at model nodes downstream of Bruntland Burn. However, because the majority of temperature loggers used in model calibration were located upstream of this point (figure 1b), it is unlikely that this will greatly affect our findings. Velocities to calibrate Heat Source's hydraulic module were calculated from the discharge–mean-velocity function developed by Tetzlaff et al. (2005a). Previous research (Garner et al. 2014; Malcolm et al.

2005) using flow accretion surveys and hydrochemical data suggest that groundwater gains along the study stretch are diffuse in nature and negligible in size; therefore, the model was run without any groundwater inputs. Heat Source requires input of a range of further hydromorphic parameters (eg. sediment thermal conductivity, % hyporheic exchange, Manning's roughness coefficient; see Bond et al. 2015 for full list). Given the difficulty associated with measuring these values in the field, or via remote sensing, they were held spatially constant and were calibrated during the model optimisation process (see section 2.4).

Stream temperatures used for model calibration were recorded by 12 TinyTag Aquatic 2 data loggers (cross-calibrated to give accuracy of ±0.02 °C) situated along the stretch (loggers G1-G12; fig 1b) and supplemented by Campbell Scientific 107 thermistor probes (accuracy of ±0.2 °C) at the Forest US and Forest DS AWS (total of 14 points). A further temperature logger (B1) installed near the mouth of Bruntland Burn (the only significant tributary present within the study stretch) was used to characterise the temperature of the tributary inflow to the Girnock Burn; all loggers/probes were installed from October 2011 to July 2013 and recorded temperature at a resolution of 15 min. Temperature loggers and probes were cross-calibrated prior to installation and housed within white PVC tubing to shield them from radiative biases. All loggers/probes were installed within the well-mixed zone to avoid possible water column stratification.

2.3.2 Tree height data

Heat Source contains routines capable of simulating the effects of riparian tree shading on radiative fluxes (and, in turn, on stream temperature) as a function of input tree height (Boyd and Kasper 2003). These routines are parameterised by supplying Heat Source with data on the height and canopy density (ie. the proportion of diffuse solar radiation blocked by the canopy) of vegetation within the riparian zone. Heat Source can also incorporate data on overhanging vegetation and vegetation growing within the channel. Heat Source subsequently uses this data to compute the reduction in radiation caused by tree cover, by partitioning H_{sw} into its direct and diffuse components (Loicq et al. 2018; Oke 1987) and computing at each model node the proportion of direct or diffuse solar radiation attenuated by the tree canopy. Full details of

the shading routines for the current model can be found in the model's source code (modified from their original formulation in Boyd & Kasper, 2003). However, in short, Heat Source computes the position of the sun relative to input riparian tree cover at each model node/timestep. For times/locations whereby the solar arc falls below the height of riparian vegetation (at a given point along the transect), the direct beam radiation is attenuated as a function of its path length through the riparian vegetation and the canopy density (using the Beer-Lambert law). Diffuse radiation is attenuated as a function of the node's 'view-to-sky' value (VTS), essentially the proportion of the hemisphere that is void of canopy; VTS is computed for each node as a function of canopy density and the angle and azimuth of vegetation at each sample point with respect to the model node.

Input tree height data are assembled using the *TTools* GIS package that accompanies Heat Source to sample a raster dataset of riparian tree heights. Heat Source also requires inputs of riparian canopy density. Although this property can be measured directly in the field, it is difficult to quantify using remote sensing or over large river corridors. The majority of stream temperature modelling studies using GIS/remote sensing approaches to obtain riparian vegetation data therefore use a look-up table approach (ie. based on tree species/age) or derive canopy density values from the literature or from sparse field estimates, with values of 40% - 100% being reported commonly (see Bond et al. 2015; Kalny et al. 2017; Loicq et al. 2018; Trimmel et al. 2016; Wawrzyniak et al. 2017; Woltemade and Hawkins 2016). Given the difficulty of estimating canopy density, we specified an initial value situated in the mid-range of literature-derived values (60%) and allowed this value to vary by ±15% during model optimisation (see Section 2.4). This approach ensured values stayed close to those commonly used for modelling stream temperatures in mixed deciduous/coniferous woodland typical of sites like Girnock Burn.

We developed three different stream temperature models. A first model was developed by parameterising Heat Source using tree heights extracted from the SfM tree height raster. This model, hereafter referred to as the 'SfM model', was used to assess the ability of SfM data to characterise spatial variability in riparian tree shading (objective 1). Spatial variability in shading was assessed by examining spatial variability in incoming solar radiation computed by Heat Source, as well as the effective shade (defined as the ratio of

potential to received solar radiation at the stream surface; Boyd and Kasper, 2003) and VTS data generated by the model. This model was also used to assess the accuracy of a stream temperature model parameterised using SfM data (objective 2); further details of model performance criteria are given in section 2.4.

To compare the accuracy of a stream temperature model parameterised with SfM data against a LiDAR-sourced model (objective 3), a second model was parameterised using a LiDAR tree height raster for the lower 1.7 km of Glen Girnock (hereafter referred to as the LiDAR model). The LiDAR tree height raster was derived by subtracting the LiDAR DTM assembled in section 2.2.2 from a LiDAR DSM generated in the same manner. Because the LiDAR data only covers the lower ~1.7 km of Girnock Burn (rather than the full 2.2 km study area), we populated the upper ~0.5 km of the LiDAR tree height map with values derived from the SfM dataset. However, because riparian tree cover is largely absent in the upper ~0.5 km of the study section, the impact of including these non-LiDAR data on stream temperature simulations was thought to be negligible. While it may have been desirable to also compare the SfM-derived shading model against one parameterised using measurements of vegetation obtained from hemispheric photography and/or clinometer data, there are currently no models that are capable of incorporating both geospatial data (eg. SfM/LiDAR) and field observations from hemispheric photography or clinometer data. Thus, it was not possible to compare these approaches in the current study. Nevertheless, given that LiDAR is widely accepted as a suitable tree height input for river temperature models (eg. Loicq et al. 2018; Justice et al. 2017; Wawrzyniak et al. 2017) and that field based data collection methods are generally more time consuming and less spatially detailed than LiDAR, we feel that the current analysis is the most useful for indicating the potential of SfM for process-based river temperature modelling.

A third Heat Source model was also developed in order to demonstrate the utility of the SfM approach for assessing the effect of riparian shading on stream temperature (objective 4). In this third instance, all tree heights were set to zero, meaning that the model was run without considering the impact of tree cover on radiative or turbulent fluxes. However, all other parameters were kept the same as the SfM/LiDAR models, allowing us to quantify the temperature difference generated by the presence/absence of tree cover. This model is hereafter referred to as the ‘no-trees model’.

2.4 Model implementation and optimisation

Heat Source was used to model stream temperatures during the same 7-day period (1 to 7 July 2013) as Garner et al. (2014). The period was characterised by relatively high air temperatures for the study site (mean, minimum and maximum of 15.6 °C, 1.3 °C and 22.0 °C respectively at the upstream-most AWS) and low flows (0.12 m^3s^{-1}). The model was run using an hourly timestep and with a spatial resolution (node spacing) of 50 m. We chose a resolution of 50 m because the greatly increased model runtime associated with finer node spacings made model optimisation impractical. However, we acknowledge that only one set of tree height samples every 50 m may lead to under- or over-representation of the true impacts of riparian shading at some model nodes. Values of air temperature, relative humidity, wind speed and bed heat flux at each model node were obtained from the nearest AWS. For solar radiation, all nodes were assigned values observed at the upstream-most AWS (ie. values in the absence of riparian shading); Heat Source's shading routine was used to generate spatially-explicit shade-corrected solar radiation values for each model node as a function of the input tree height raster.

Heat Source (parameterised with the SfM tree heights data) was calibrated to stream temperatures observed within the 2.2 km stretch by adjusting model parameters (see table 1) to minimise model root mean square error (RMSE) between observed and simulated stream temperatures at each of the 14 water temperature observation sites. Although Heat Source allows model parameters to vary spatially, we used a fixed set of parameters to reduce model calibration/optimisation time. Model calibration was achieved by manually adjusting calibration parameters to explore the range of parameters that generated reasonable RMSE results while permitting simulated heat fluxes and velocities to stay within real world values. Thereafter, Latin hypercube sampling was used to generate 5000 unique parameter combinations from across the parameter space defined by these limits, and a Monte Carlo-type approach used to find the parameter combination that minimised RMSE against the 14 observation sites (see table 1 for optimised parameter set). The parameter set that produced the optimal RMSE was thus selected. Following this initial model optimisation phase, Heat

Source was re-run three times using the different tree height models described in section 2.3.2; these models were subsequently quantified in terms of their RMSE, bias and simulated temperature.

Table 1. Parameter set for optimised model of Girnock Burn

Parameter	Units	Value
Sediment thermal conductivity	$W\ m^{-1}\ °C^{-1}$	1.14
Sediment thermal diffusivity	$m^{-2}\ s^{-1}$	6.40×10^{-3}
Sediment porosity	unitless	0.40
Manning's roughness coefficient	$s^{-1}\ m^{1/3}$	0.71
Thickness of hyporheic layer	m	0.39
Hyporheic exchange	%	4.83
Wind function coefficient *a*	$mb^{-1}\ m\ s^{-1}$	2.94×10^{-9}
Wind function coefficient *b*	mb^{-1}	1.20×10^{-9}
Deep alluvium temperature	°C	9.00
Canopy density	%	72.38

3. Results

3.1 SfM-derived shading data

Figure 4a highlights spatio-temporal variability in incoming shortwave radiation received at the stream, as computed from the SfM-parameterised Heat Source model. While temporal variability in incoming solar radiation is typical of the diurnal insolation cycle (y-axis), the spatial (downstream) dimension is more irregular indicating the presence of substantial tree shading within these reaches (x-axis). This is summarised in the effective shade data yielded by Heat Source, which indicates that the SfM approach is capable of characterising the considerable spatial variability in shading that exists along the 2.2 km study stretch (figure 4b). The view to sky data generated by Heat Source shows matching, but dampened, trends (figure 4c). This reduced variability in VTS in comparison to effective shade is due to the fact that VTS integrates tree cover across the entire hemisphere, whereas the effective shade data characterises the specific impact shading has on the amount of solar radiation received as the sun travels across its arc.

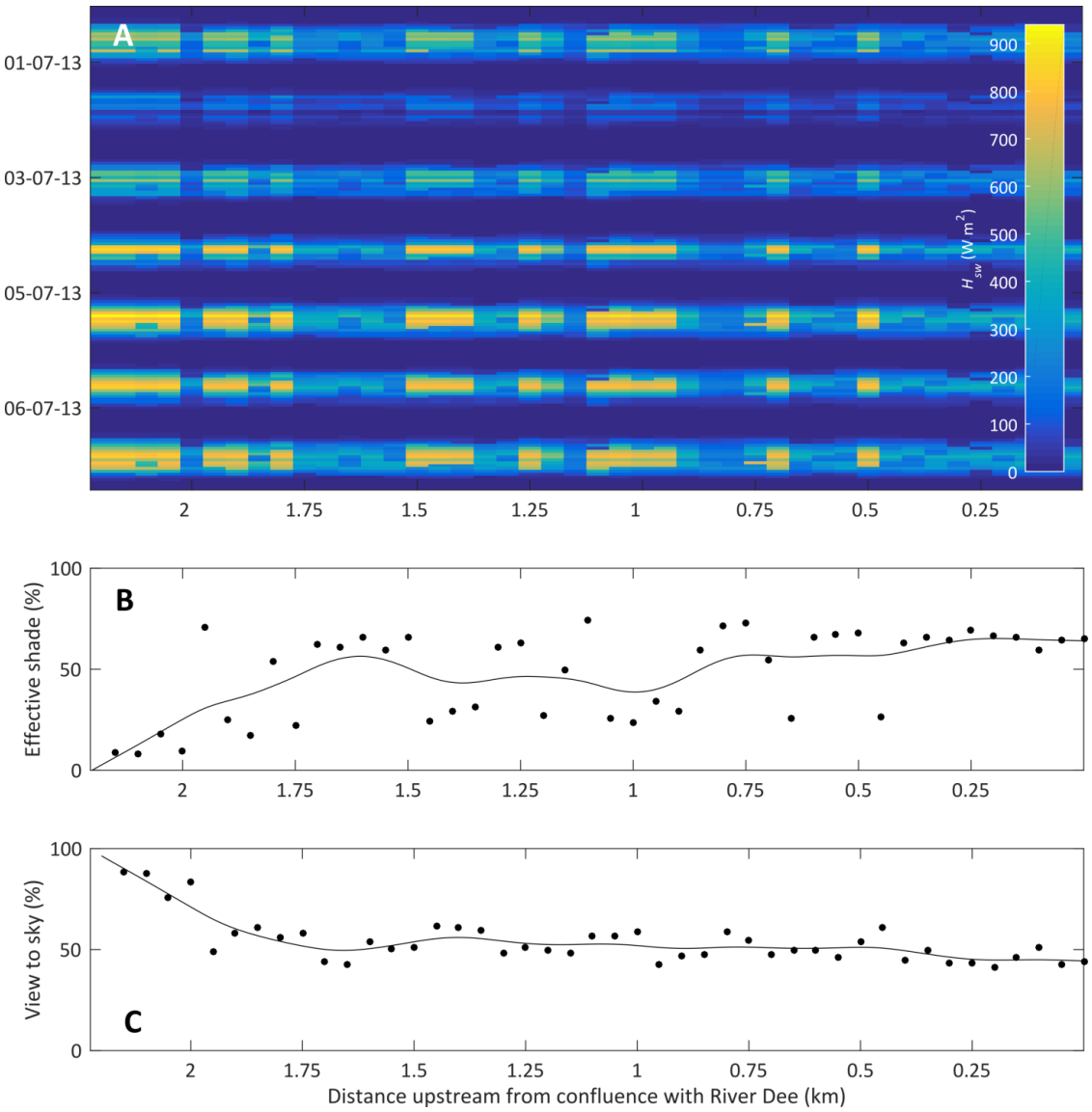

Figure 4. Variability in a) computed H_{sw} received at the stream surface following application of Heat Source shading routines to SfM-derived tree heights, b) time-averaged effective shade and c) view to sky (VTS). Solid lines in b) and c) indicate LOESS-smoothed average effective shade and VTS

Comparison of the shading data (figure 4) with the SfM-derived orthophoto and tree height raster (figure 2a and 2d) explains downstream variability in shading. As expected, shade is generally lowest (<10%) at the upstream-most model nodes (2.2 – 1.9 km), corresponding to the open moorland section of Girnock Burn where riparian vegetation is sparse with the exception of a few individual trees. Effective shade increases (~40 - 50%) as the Girnock Burn enters an area of more consistent forest cover (tree heights ≈ 5 – 15 m) between 1.85 and 1.5 km downstream, before reducing slightly (20 – 30%) between 1.45 and 0.9 km. Here, the reduction in effective shading coincides with a decrease in forest density where the river is oriented S-N

followed by an increase in channel width associated with diminished riparian overhang. Shade increases (60-70%) as the stream re-enters a densely wooded reach (0.85 - 0 km), characterised by a SW-NE orientation and greater tree heights (15-25 m). This downstream-most reach generally exhibited the highest effective shade/VTS and lowest computed solar radiation.

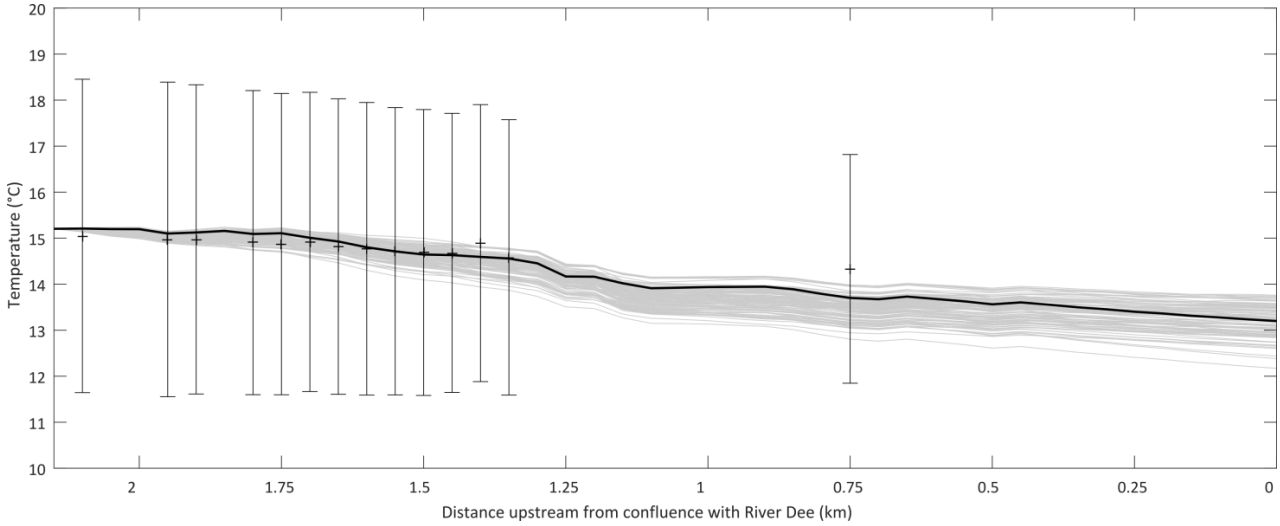

Figure 5. Time-averaged river temperature long profile for 100 best optimisation runs (based on RMSE). Best model (lowest mean RMSE) given by thick black line. Vertical bars give standard deviation of temperatures observed at logger sites; crosses give mean recorded river temperature.

3.2 SfM model performance and simulated temperature patterns

Temperatures simulated by the SfM model are close to those observed by loggers installed in the lower Girnock Burn. The high degree of similarity (±0.5 °C) between the 100 'best' optimisation runs (fig 5) indicates relatively low uncertainty in the optimised parameter set. RMSE computed between the optimal model and the 14 temperature observations sites (including logger G12) indicates that the SfM model performs well (RMSE ≈ 0.18 – 0.69 °C; table 2). The general pattern of increasing RMSE in a streamwise direction is to be expected, as a function of the propagation of minor errors resulting from model calibration inadequacies with increasing distance from the upstream boundary condition. Bias in simulated temperatures indicates a weak over prediction (0.12 °C) compared to the observed data. Closer inspection of the temperature series reveals that the model tends to over-estimate daytime peak temperature and (to a lesser extent) under-predict night-time lows (figure 6). This is the case especially on 2nd July, when the low simulated temperature

in comparison to observed values likely relates to the model's inability to represent advective inputs from a small rainfall event on this day. These biases may also result from inadequacies in the parameterisation of Heat Source's hydraulic model component leading to under- or overestimates in the stream surface width (and thus, the energy exchange surface). Nevertheless, the low RMSE and bias indicate that the model is capable of simulating temperatures in Girnock Burn with a similar degree of accuracy to related studies (see section 4.2).

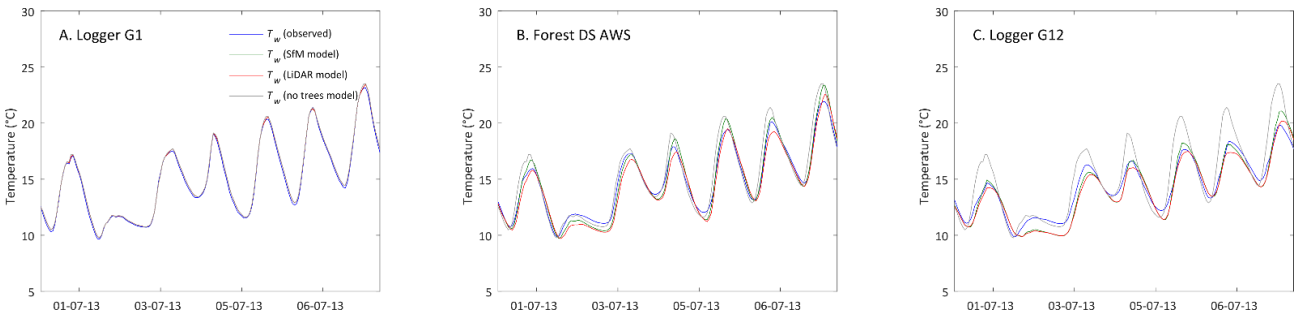

Figure 6. Observed vs. simulated (SfM, LiDAR and no trees models) stream temperature at a) upstream, b) mid-stream and c) downstream logger sites. Note that simulations for SfM and LiDAR models at logger G1 are identical.

Table 2. Model performance metrics for SfM and LiDAR models across all temperature observation sites

	SfM model		LiDAR model		No trees model	
Site	RMSE	Bias	RMSE	Bias	RMSE	Bias
G1	0.18	0.15	0.18	0.15	0.19	0.16
G2	0.31	0.17	0.31	0.17	0.35	0.25
G3	0.32	0.19	0.32	0.19	0.42	0.27
G4	0.47	0.24	0.47	0.24	0.62	0.38
G5	0.46	0.21	0.46	0.21	0.70	0.42
Forest US AWS	0.42	0.12	0.42	0.11	0.73	0.39
G6	0.46	0.14	0.46	0.14	0.87	0.51
G7	0.51	0.14	0.51	0.14	0.97	0.57
G8	0.58	0.15	0.57	0.15	1.05	0.62
G9	0.51	0.16	0.49	0.01	1.10	0.63
G10	0.55	0.15	0.53	-0.02	1.16	0.63
Forest DS AWS	0.53	-0.09	0.62	-0.32	1.09	0.40
G11	0.58	0.22	0.52	-0.01	1.27	0.71
G12	0.69	-0.23	0.71	-0.41	1.57	0.64
Mean	0.47	0.12	0.47	0.05	0.86	0.47

Both observed and simulated stream temperatures reflected a general trend of instantaneous downstream temperature reductions within the study stretch, with a time-averaged downstream temperature gradient of -0.7 °C km^{-1} over the study period (figure 7). However, closer inspection of the simulated temperatures reveals finer-scale spatial patterns. While the time-averaged temperature decrease over the upstream-most nodes (2.2 – 1.8 km) is relatively low (corresponding to lower riparian tree shading in this section), the rate of temperature decrease downstream of this section is more pronounced until approximately 1.3 km, where the cool input from Bruntland Burn yields a large temperature drop that persists downstream over several model nodes. Stream temperature is relatively stable between 1.25 and 0.9 km, but the negative temperature trend re-asserts over the downstream-most 900 m (up to the confluence with the River Dee), coinciding with the tallest/densest riparian vegetation. The downstream temperature trend exhibits strong diurnal variability (figure 8a), whereby the negative downstream trend persists during the daytime but is replaced by a weak positive signal during the night. The greatest instantaneous negative trend in temperature between the upstream- and downstream-most model nodes (-5.4 °C) was observed at 13:00 on 7 July 2013, while the largest instantaneous temperature increase (1.8 °C) was observed at 04:00 on 6 July 2013 (figure

8b). These values equate to minimum and maximum instantaneous downstream temperature gradients of -2.5 and 0.8 °C km^{-1} respectively.

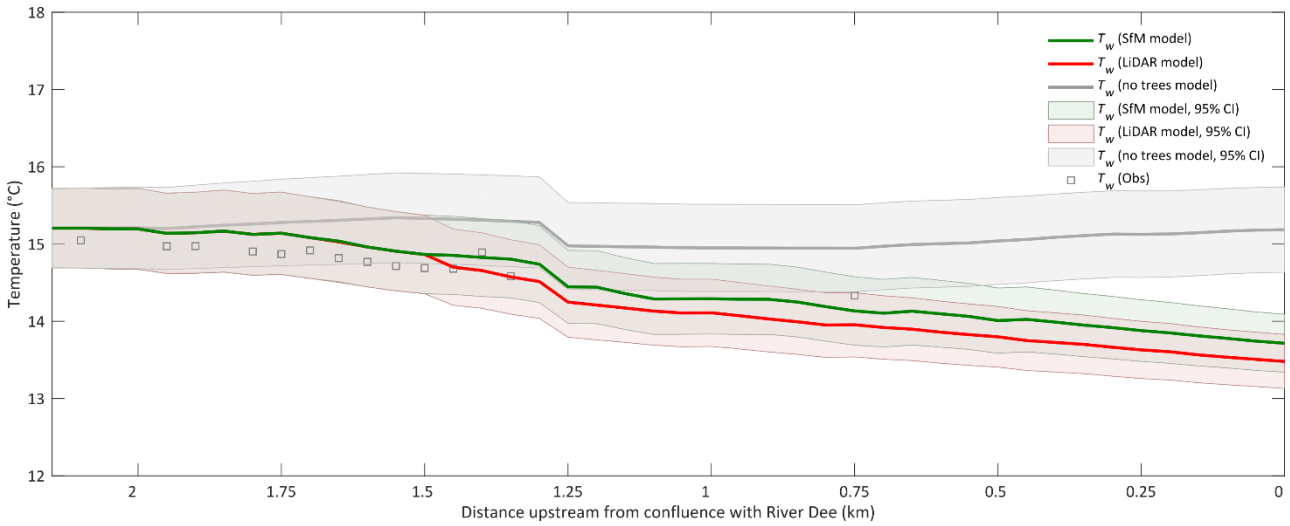

Figure 7. Time-averaged temperature long profiles for Girnock Burn simulated with SfM model (green line), LiDAR model (red line) and no trees model (grey line). Shaded area represents 95th percentiles around mean. Note that simulations for the SfM and LiDAR models upstream of 1.7 km are identical.

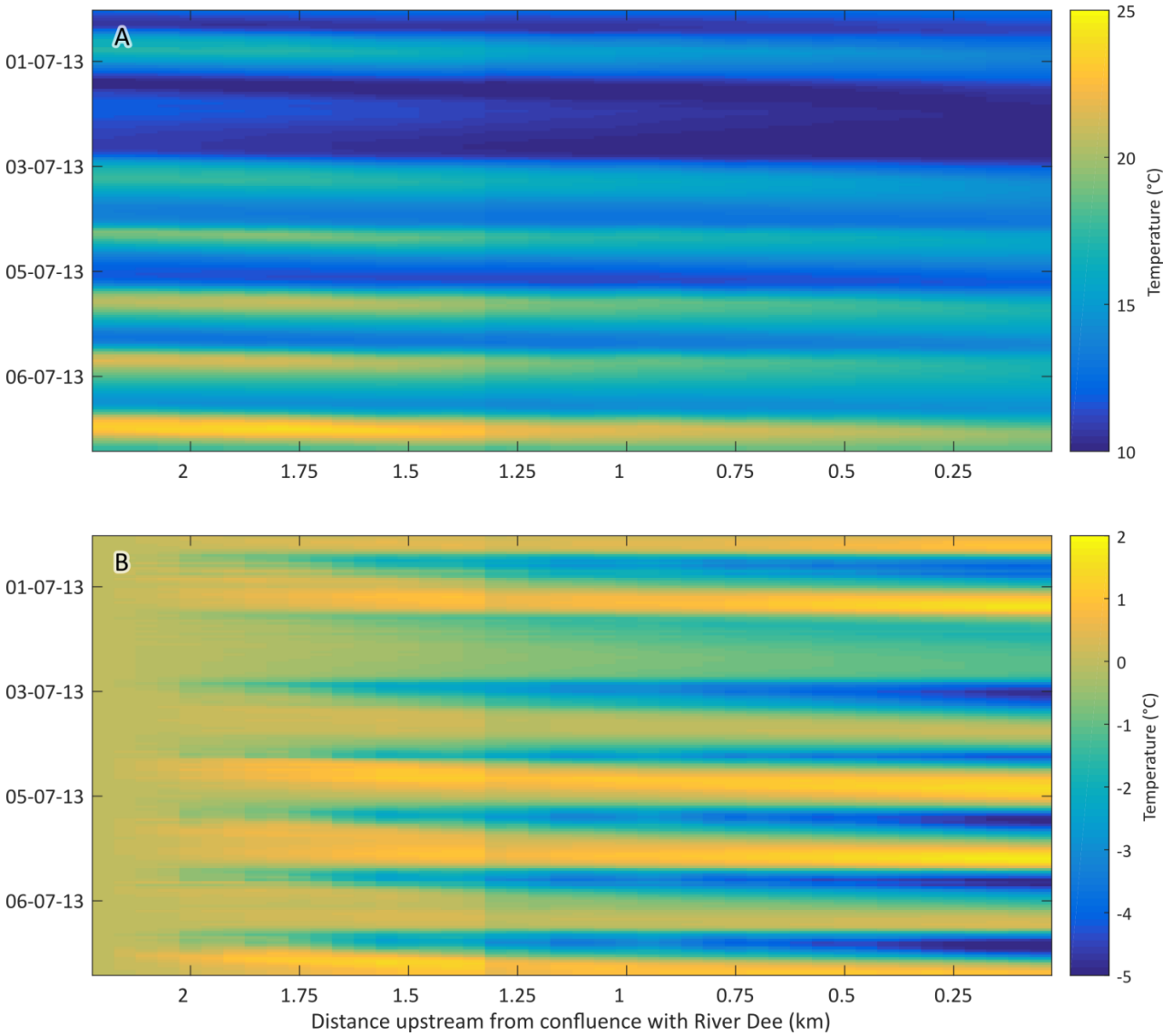

Figure 8. Spatio-temporal variability in simulated water temperature for SfM model showing a) absolute temperature and b) instantaneous difference between 1st and nth model node.

3.3 Comparison of SfM and LiDAR models

Average RMSE yielded by the LiDAR model was almost identical to that of the SfM model (both equal to 0.47 °C), suggesting that the performance of a stream temperature model parameterised using SfM data is broadly comparable with one parameterised using a more conventional LiDAR approach (table 2). Indeed, the difference in reach-averaged RMSE between the two models was less than 1/1000th of a degree over the entire study period. Mean bias of the LiDAR model (0.05 °C) was lower (ie. better) than that of the SfM model

(0.12 °C), corresponding to a reduction in the (minor) systematic overprediction exhibited by the SfM model in the lower reaches of Girnock Burn. However, the difference between the models is nonetheless small.

Closer inspection of figures 6 and 7 indicates that while the SfM model tends to overestimate daytime peak temperatures (and underestimate nighttime lows), peak temperatures estimated by the LiDAR model are generally closer to observed data (although night time lows are still underestimated). This results in a model which is on average 0.22 °C cooler than that of the SfM model (figure 7; calculated for nodes downstream of 1.7 km). The slightly reduced temperature of the LiDAR model is likely a function of bias in the SfM DTM ground heights. This means that that calculated tree heights are marginally higher in the LiDAR model, leading to a systematic reduction in the computed radiative flux reaching the stream surface. However, the fact that the difference in temperature between the two models stays relatively constant as a function of distance downstream indicates this systematic bias is very small, leading to little substantial downstream differences in shading. More localised variability in simulated temperature between the two models is likely a result of small differences in computed tree height resulting from the difference in acquisition date between the SfM and LiDAR datasets.

3.4 Quantifying the effect of riparian woodland on stream temperature

The space-time averaged difference in simulated temperatures between the SfM and no-trees models indicates that riparian tree cover drives a mean 'cooling' effect of ~0.66 °C in the lower Girnock Burn. Although this suggests that riparian shading has a relatively minor (ie. <1 °C) impact on stream temperature, inspection of the temperature time-series (figure 6) reveals notable temporal variability in the magnitude of this shading effect. Indeed, the no-trees model yields much higher daytime maxima (study period mean of 3.3 °C warmer) at the downstream-most model node. This indicates that in the absence of tree cover, peak stream temperature in the lower reaches of Girnock Burn would be increased substantially during the daytime. Furthermore, the timing of daily temperature maxima/minima is shifted in comparison to the SfM model, with daytime highs/night-time lows occurring on average 130 and 50 minutes earlier respectively.

In terms of spatial temperature patterns, the no-trees model suggests an extremely weak time-averaged downstream negative temperature trend (-0.001 °C km^{-1}). However, closer inspection of the simulation (figure 7) indicates that this longitudinal pattern is very dependent on cool water inputs from the Bruntland Burn at 1.3 km, with reaches up- and downstream of this point (2.2 km – 1.35 km and 0.75 – 0 km) showing positive downstream temperature gradients (0.1 °C km^{-1} and 0.2 °C km^{-1}) of the magnitude commonly associated with unshaded reaches. Excluding the influence of Burntland Burn, the no-trees model generated a consistent increasing temperature trend that contrasts with the SfM model, especially in the downstream-most reaches (figure 7).

4. Discussion

4.1 Utility of SfM for parameterising process-based temperature models of shade-impacted rivers

SfM represents a cost-effective solution for obtaining spatially detailed tree height data to parameterise shading routines in process-based river temperature models. Collection of the sUAS and field data necessary for the development of the SfM tree height raster took approximately two days (two fieldworkers present), with a further 3-4 days (not including computer runtime) necessary for the generation of the SfM dataset. Following refinement of the workflow, we believe that the SfM processing could be further reduced to 1-2 days' work. While we acknowledge that prerequisite training in sUAS and SfM software use is required, we believe that this still represents a substantial time and cost saving in comparison to traditional field approaches for characterising riparian shading, given that the costs of lab/office work (ie. SfM processing) are generally much lower than those of fieldwork. Indeed, the acquisition of hemispheric photography of the same section of Girnock Burn at a streamwise resolution approaching that of our SfM dataset (eg. Garner et al, 2014) took considerably longer (>1 week), with several days' additional office work still needed for image processing. Conversely, while it may be feasible to obtain numerous coarsely-spaced laser or clinometer measurements of riparian tree heights in a similar time window to that needed for SfM data acquisition, the spatial resolution of such measurements would still be of several orders of magnitude lower than that of SfM,

and the accuracy of such observations may also not be substantially improved, given the error and operator bias that is commonly associated with such field instruments (eg. Williams et al. 1994; Larjavaara et al. 2013). Given that river scientists and managers increasingly have access to (and proficiency in) technologies such as sUAS and SfM, our proposed approach represents a substantial time/cost saving in comparison to these 'conventional' field techniques, while providing data of a comparable accuracy at much higher resolution.

In addition to its potential for reducing the costs associated with fieldwork in remote locations, the high degree of spatial variability present within the Heat Source shading outputs demonstrates the capacity of SfM to characterise fine-scale patchiness in riparian shading. This, coupled with the good model performance metrics (eg. RMSE < 0.7 °C) confirms SfM as a viable method for parameterising riparian shading routines in a process-based temperature model. Indeed, the SfM-parameterised model produced very similar performance metrics (RMSE, bias) to the model parameterised using high quality 'conventional' LiDAR tree heights, indicating that the SfM approach is able to reproduce riparian shading (and thus, model stream temperatures) with a level of accuracy approaching this more commonly applied technique.

Despite these promising results, the cost and benefits of these two techniques depends heavily upon the spatial scale of a given study. sUAS-based SfM is well adapted to the generation of reach-scale (10^0 km) tree height datasets, and is thus ideally suited for use in small streams where the acquisition of LiDAR data is not cost effective. However, the acquisition of sUAS-based data becomes increasingly challenging as the size of the study area increases due to legal (line of sight flights, requirement for exclusion around people and property) and logistical (flight times and battery life) constraints. For larger (10^1 - 10^2 km) studies, there will inevitably be a point at which LiDAR-based techniques may prove more appropriate or cost effective for characterising tree heights over entire river corridors. Nonetheless, previous studies have demonstrated the utility of SfM for assembling whole river-scale topographic datasets (eg. Dietrich 2016) from conventional airborne remote sensing platforms, meaning that SfM still represents a viable solution for generating riparian shading data at 10^1 - 10^2 km scales. Furthermore, in rivers across the UK and Europe where forest cover is often patchy and discontinuous, several sUAS-based SfM surveys of smaller afforested reaches are still likely to cost less than one LiDAR survey of an entire river. In addition, SfM lends itself well to temporal monitoring,

potentially allowing for the incorporation of seasonally variable shading in river temperature models or assessment of the long-term effects of riparian tree planting activities. The ability to rapidly generate riparian shading data could aid change detection following forest harvesting or forest fires. Taken together, these findings emphasise the utility of SfM for river scientists and managers looking to a) understand how spatial/temporal variability in shading impacts stream temperature and b) inform strategies for optimal riparian planting to reduce impacts of future climate change.

4.2 Comparison to previous temperature modelling studies in Girnock Burn

Results of both our SfM and LiDAR models are very similar to the findings of previous river temperature modelling studies in Girnock Burn (Garner et al. 2014; 2017b; Fabris et al. 2018). Indeed, the simulated spatio-temporal distribution of stream temperatures support the findings of Garner et al. (2014, 2017b) and Fabris et al. (2018) who noted the presence of an instantaneous negative downstream temperature trend within the Girnock Burn during the daytime. This trend resulted from a combination of a) cool water advected from upstream, and b) greatly reduced net energy gain in comparison to open reaches (Garner et al. 2017b). Although our study simulated slightly higher magnitude negative (daytime) and positive (night-time) temperature gradients (-2.5 °C km^{-1} and 0.8 °C km^{-1}) than those reported by Garner et al. (2014; -2.4 °C km^{-1} and 0.5 °C km^{-1}), it is likely that this disparity results from the advective input from the Bruntland Burn which is downstream of the study reach in Garner et al. (2014). Indeed, when limiting our comparison to the same reach used in their study, the negative downstream temperature gradient (-2.4 °C km^{-1}) simulated by our model was identical. However, our model did produce a notably higher night-time temperature increase (1.2 °C km^{-1}) over this reach; it is possible that parameter uncertainty pertaining to turbulent and longwave heat fluxes (which dominate night-time heat exchanges; Hannah et al., 2008) is responsible for this discrepancy. Similar to all remote sensing and modelling studies, the approaches used within this investigation are simplifications of reality and as such, inaccuracies resulting from model parameterisation uncertainty are expected. For a detailed discussion of potential error arising from a) uncertainty in input meteorological data, b) bed/hyporheic energy flux estimates and c) flow accretion/groundwater inputs see Garner et al. (2014;

2017). Nevertheless, the similarity in spatio-temporal temperature patterns between our investigation and previous process-based modelling studies of Girnock Burn indicates that the SfM model is performing well.

The models presented in this study, parameterised using an SfM tree height raster, compare favourably to previously published approaches where shortwave radiation was scaled using more traditional and time-consuming methods of canopy characterisation. Garner et al. (2014) developed a process-based river temperature model that used spatially-explicit hemispheric photography of the riparian canopy to simulate the effects of riparian shading on stream temperatures. They reported model RMSE values of 0.2 – 0.4 °C for the section of Girnock Burn corresponding to the upper 1050 m of our study stretch. More recently, Fabris et al. (2018) applied a different approach, using GIS polygons to characterise the locations of riparian woodland, reducing H_{sw} at model nodes falling within these polygons by a parameterised coefficient to approximate the effects of shading on solar radiation. They reported a mean RMSE of 0.7 °C for four temperature observation sites covering a ~4 km section of the stream. The mean RMSE of 0.47 °C reported in our study compares well to these investigations; furthermore, when focusing on the same reach as Garner et al. (2014), mean RMSE (0.45 °C) is only marginally poorer. Given that temperature simulations in Garner et al. (2014) were generated using an extremely highly resolved (5 m) river temperature model incorporating detailed hemispheric photography and geomorphological data, these results are extremely promising in light of our model's much reduced resolution (50 m), and further emphasise the potential utility of the SfM approach for characterising the spatially-explicit effects of tree shading on stream temperature.

Spatial variability in the SfM-derived effective shade/VTS data (fig 4) was consistent with the findings of a range of recent studies (eg. DeWalle 2008; 2010; Garner et al. 2017b; Li et al. 2012) demonstrating that channel orientation is a key determinant of riparian shading and thus the effectiveness of riparian woodland in reducing river temperature. Li et al. (2012) found that variability in tree height and overhang only significantly affected E-W oriented streams, while Garner et al. (2017b) simulated riparian shading under a range of channel orientations and forest densities, and found that S-N aligned channels only provide substantial shading when forest cover is very dense and overhangs the channel. Similarly, DeWalle (2010) noted that substantially wider riparian buffers were needed to produce shade in S-N oriented streams. This,

in combination with a reduction in overhanging vegetation (which has a proportionally greater effect in small streams; DeWalle, 2008) presumably explains why effective shade/VTS in our model is substantially reduced between 1.45 and 1.2 km, where the combination of an S-N aligned channel and a single strip of riparian cover only generated a small amount of shading in relation to the more densely forested S-N aligned reach immediately upstream. Similarly, the increase in effective shade/VTS towards the downstream-most end of the study stretch (0.85 km to confluence) is likely due in part to the change in orientation from S-N to SW-NE, which leads to increased shading over the course of the day given the position of the solar arc in comparison to the river channel (see Garner et al. 2017b). Our findings therefore further emphasise the importance of channel orientation (in addition to residence time, width, forest height, density and overhang; eg. Li et al. 2012) in controlling riparian shading and thus, stream temperature.

4.3 Towards a better understanding of the effect of riparian woodland on stream temperature

The paired 'trees/no-trees' modelling approach detailed here allowed us to quantify the effect of riparian woodland, ie. the amount by which riparian vegetation moderates stream temperatures in the Girnock Burn. Inspection of the no-trees model simulations indicates that, in the absence of riparian shading, peak daytime temperature in the lower reaches of Girnock Burn would have been an average of 3.3 °C warmer during the study period. Notably, without tree cover, Girnock Burn could have exceeded the upper growth limit for juvenile Atlantic salmon (~23 °C; Elliot and Elliot, 2010; Breau et al. 2007; Dugdale et al. 2016) for several hours during the study period, potentially leading to thermoregulatory behaviour among salmonids resident within the stream. Given that river managers in some parts of the UK and Europe are actively involved in the removal of riparian woodland (CASS 2010) with the stated aim of improving salmonid productivity (to increase mean temperature in cool reaches or to improve other habitat characteristics such as invertebrate taxonomic richness), these results emphasise the importance of running similar paired-model approaches prior to riparian deforestation to ensure that the importance of riparian woodland to the stream's thermal regime is appropriately quantified.

While the ability of riparian woodland to moderate stream temperature extremes has been known for some time (eg. Brown and Krygier 1970; Moore et al. 2005a; Rishel et al. 1982), further information is needed regarding the exact environmental settings under which riparian woodland generates greatest reductions in stream temperatures (Garner et al. 2017). We suggest that the low cost and good performance of the SfM methodology described here is ideally suited for addressing this key knowledge gap using similar modelling approaches to the presented here, applied systematically across a larger geographic and environmental range. By acquiring riparian tree height data from a series of different rivers and repeating our trees/no-trees modelling strategy at each location, it should be possible to gain an improved understanding of the impacts of riparian woodland on stream temperature across a range of different environmental settings (ie. varying woodland species composition, geomorphology and hydrogeology). Such information would not only help inform climate change adaptation strategies for temperature-impacted watersheds, but would also help in the development of best-practise strategies to ensure that riparian tree planting is prioritised to areas where it will have the greatest impact on stream temperature. Thus, the SfM modelling approach represents an encouraging methodology with which to systematically assess riparian woodland effects on stream temperature at intermediate scales in a way that has not been previously possible owing to the high costs (eg. LiDAR, hemispheric photography) or low accuracy (eg. GIS polygons) of alternative sources of riparian shading data.

4.4 Limitations and future work

Despite these promising results, it is necessary to discuss potential limitations arising from our approach. One potential disadvantage of SfM for the characterisation of riparian shading is its limited ability to measure ground elevation beneath dense forest canopies. This has implications for the derivation of 'bare earth' digital terrain models needed for tree height calculation. In this study, there were sufficient canopy gaps that many ground points were present in the SfM point cloud. This allowed for the generation of a 'bare earth' DTM with an acceptable level of accuracy (RMSE = 1.25 m) for the derivation of tree heights through DSM – DTM subtraction. In more dense (particularly commercial conifer; eg. Dugdale et al. 2018) forests, SfM may

not be able to generate enough ground points for the derivation of a DTM of reasonable accuracy. In such cases, it may be possible to derive a 'bare earth' DTM from other remote sensing products (eg. radar, photogrammetry) or conventional topographic surveys, which could introduce further errors into tree height estimates. Researchers/managers attempting to use SfM to characterise riparian tree heights should be aware of this potential limitation of the technique.

The difficulty in resolving ground elevations has implications for the characterisation of riparian canopy density needed for the diffuse shading routines of Heat Source or similar models (see Dugdale et al., 2017). In true LiDAR forestry applications, canopy density can be estimated as the ratio of ground to canopy LiDAR returns (Lee and Lucas 2007; Lim et al. 2003). Although this technique has also been successfully applied to SfM datasets in sparse agriculture/agroforestry contexts (Mathews and Jensen 2013; Messinger et al. 2016; Wallace et al. 2016), this method is not as readily applicable to (semi-) natural multi-species forest stands such as that present in Glen Girnock. Furthermore, while LiDAR data does exist for the lower stretch of Girnock Burn, it was acquired relatively early in the growing season, and the extraction of canopy density from 'leaf-off' LiDAR data is prone to complications (Bachiller-Jareno et al. 2019). Instead, we supplied Heat Source with a literature-derived estimate of canopy density (subsequently refined during model optimisation) to compute the attenuation of the diffuse solar radiation component through the riparian canopy. Although the use of literature-derived estimates of canopy density in this manner is by no means uncommon amongst river temperature modelling studies (even amongst those which used LiDAR to compute vegetation height; Loicq et al. 2018; Wawrzyniak et al. 2017), it is nonetheless suboptimal compared to real data on canopy density. Therefore, it is pertinent to note that such an approach may yield under- or over-estimates of the true impact of riparian vegetation on diffuse shortwave fluxes. Potential solutions to this issue include hybrid approaches combining SfM-derived tree heights with limited hemispheric photography surveys and/or data from lookup-tables. However, these solutions would both require significant model development (and validation prior to application). Alternatively, recent advances in drone-based forestry applications indicate that 'common' forest properties such as leaf area index (LAI), leaf volume and even tree species are now obtainable from sUAS-based approaches (Alonzo et al. 2018; Jensen and Mathews 2016; Mathews and Jensen 2013; Michez et al. 2016; Roth et al. 2018; Tang and Shao 2015). Given that Heat Source

already contains routines capable of estimating diffuse solar radiation attenuation as a function of LAI and extinction coefficient (*k*), it is possible that such approaches could be applied to the current model to refine the estimated radiative flux under tree-lined reaches and thus improve simulated temperatures. We therefore advocate future diffusometry work to compare diffuse radiative fluxes computed under these contrasting approaches.

A more complex solution to both of these problems would be to use SfM to generate a 'true' 3D model of the riparian tree canopy (rather than the '2.5D' digital elevation data used in this study) by flying both under and over the tree canopy, or by integrating the SfM-derived tree canopy model with below-canopy data from a terrestrial laser scanner or even selective hemispheric photography. Such a dataset would allow for the detailed characterisation of canopy structure and density (including digital representations of individual branches and leaves). By combining such data with advanced riparian shading routines (eg. DeWalle 2010; Li et al. 2012; Rutherford et al. 2018a) or even ray tracing methods common to computer vision (eg. Bittner et al. 2012), it may be possible to arrive at a highly accurate representation of the complex interaction between incoming solar radiation, riparian tree shading, and river temperature heterogeneity. However, such a study would require significant investment in fieldwork, field equipment and computing power, putting it beyond the remit of many river scientists and managers for whom simpler models such as Heat Source normally suffice.

Our model focused on a relatively short time series when water temperature in Girnock Burn was high and there were few significant inputs of precipitation to the model. The decision to focus on this period was predicated upon the fact that we wanted to directly compare our modelling approach to the results of Garner et al. (2014) who simulated temperatures for the same period. In doing so, we demonstrate that our approach provided simulations of a similar degree of accuracy to a model incorporating much higher resolution hemispheric photography-derived measurements of riparian shading. However, we acknowledge that this short modelling period limits our ability to determine the performance of the model over longer simulation periods. Indeed, while we assume that our model would perform similarly well during other periods with analogous hydrometeorological conditions, its performance during other seasons or especially

under periods of persistent rainfall is currently unknown. Inspection of figure 6 indicates the existence of possible negative biases during cooler, high-precipitation conditions. Future research will therefore focus on achieving model calibration during longer time periods incorporating increased hydrometeorological variability, with a view to further refining simulated stream temperature.

5. Conclusion

This paper has demonstrated that drone-based SfM mapping can provide an accurate and detailed spatial representation of riparian tree cover that can be used to parameterise shading routines in process-based river temperature models. The results illustrate that the combination of SfM data and process-based temperature models are capable of characterising fine-scale variability in riparian shading and that temperature simulations incorporating this shading are of comparable accuracy to those achieved using either 'conventional' LiDAR data or previous studies parameterised using ground-based measurements of canopy density. Taken together, these findings highlight SfM as a viable tool for parameterising temperature model shading routines, particularly in small streams or river environments comprising patchy or inconsistent tree cover where more conventional approaches are too costly (eg. LiDAR) or too coarse (eg. GIS polygons) for accurate shading representation. By comparing our SfM-derived (tree cover) stream temperature model to a model without tree cover, we also demonstrate the extent to which riparian shading moderates stream temperatures in the Girnock Burn. We advocate the use of similar modelling approaches in other locations to better understand fundamental heat exchange process and controls, which may underpin assessment of optimal riparian tree planting for stream temperature outcomes. In light of the relative ease with which this sUAS-based SfM data can be obtained, we believe that the approach detailed herein represents a practical solution to the acquisition of riparian tree height data for headwater areas and for locations where LiDAR surveys are infeasible. Given the threat posed by climate change to river ecosystems, the ability to a) better characterise riparian shading in rivers and b) better understand the effects of woodland on stream temperature across multiple locations is likely to be valuable for developing riparian land management strategies to mitigate river thermal degradation.

6. Acknowledgements

This project has received funding from the European Union's Horizon 2020 research and innovation programme under Marie Skłodowska-Curie Grant Agreement No. 702468. IAM's contribution forms part of Marine Scotland Service Level Agreement FW02G. We wish to acknowledge the invaluable support of Stephen McLaren, Pauline Proudlock, Karen Millidine, Faye Jackson and Ross Glover of Marine Scotland Science. We would also like to thank the Abergeldie and Balmoral estates for permission to conduct the sUAS surveys. Grace Garner kindly provided the weather station and temperature logger data collected during her PhD project (available at http://doi.org/10.7489/12109-1). Thanks also to Ryan Michie (Oregon Department of Environmental Quality) for advice regarding the implementation of Heat Source. The LiDAR data used for SfM validation is Crown copyright Scottish Government, SEPA and Scottish Water (2012); Open Government Licence (http://www.nationalarchives.gov.uk/doc/open-government-licence/) and is available from the Scottish Remote Sensing Portal (https://remotesensingdata.gov.scot).

7. References

Agisoft (2017). *Photoscan Professional*. Version 1.3.5 build 5067. St. Petersburg, Russia: Agisoft LLC

Alonzo, M., Andersen, H.-E., Morton, D.C., & Cook, B.D. (2018). Quantifying Boreal Forest Structure and Composition Using UAV Structure from Motion. *Forests*, 9, 119

Bachiller-Jareno, N., Hutchins, M.G., Bowes, M.J., Charlton, M.B., & Orr, H.G. (2019). A novel application of remote sensing for modelling impacts of tree shading on water quality. *Journal of Environmental Management*, 230, 33-42

Baker, E.A., Lautz, L.K., Kelleher, C.A., & McKenzie, J.M. (2018). The importance of incorporating diurnally fluctuating stream discharge in stream temperature energy balance models. *Hydrological Processes*, 32, 2901-2914

Birdal, A.C., Avdan, U., & Türk, T. (2017). Estimating tree heights with images from an unmanned aerial vehicle. *Geomatics, Natural Hazards and Risk,* 8, 1144-1156

Bittner, S., Gayler, S., Biernath, C., Winkler, J.B., Seifert, S., Pretzsch, H., & Priesack, E. (2012). Evaluation of a ray-tracing canopy light model based on terrestrial laser scans. *Canadian Journal of Remote Sensing*, 38, 619-628

Bond, R.M., Stubblefield, A.P., & Van Kirk, R.W. (2015). Sensitivity of summer stream temperatures to climate variability and riparian reforestation strategies. *Journal of Hydrology: Regional Studies, 4, Part B*, 267-279

Bowler, D.E., Mant, R., Orr, H., Hannah, D.M., & Pullin, A.S. (2012). What are the effects of wooded riparian zones on stream temperature? *Environmental Evidence*, 1, 3

Boyd, M., & Kasper, B. (2003). *Analytical methods for dynamic open channel heat and mass transfer: Methodology for Heat Source model version 7.0*. Portland, OR: Oregon Department of Environmental Quality, 193 p

Brown, G.W., & Krygier, J.T. (1970). Effects of Clear-Cutting on Stream Temperature. *Water Resources Research, 6*, 1133-1139

Carbonneau, P.E., & Dietrich, J.T. (2017). Cost-effective non-metric photogrammetry from consumer-grade sUAS: implications for direct georeferencing of structure from motion photogrammetry. *Earth Surface Processes and Landforms, 42*, 473-486

Chen, Y.D., Carsel, R.F., McCutcheon, S.C., & Nutter, W.L. (1998a). Stream Temperature Simulation of Forested Riparian Areas: I. Watershed-Scale Model Development. *Journal of Environmental Engineering, 124*, 304-315

Chen, Y.D., McCutcheon, S.C., Norton, D.J., & Nutter, W.L. (1998b). Stream Temperature Simulation of Forested Riparian Areas: II. Model Application. *Journal of Environmental Engineering, 124*, 316-328

Comte, L., Buisson, L., Daufresne, M., & Grenouillet, G. (2013). Climate-induced changes in the distribution of freshwater fish: observed and predicted trends. *Freshwater Biology, 58*, 625-639

Cox, M.M., & Bolte, J.P. (2007). A spatially explicit network-based model for estimating stream temperature distribution. *Environmental Modelling & Software, 22*, 502-514

Davies-Colley, R.J., & Payne, G.W. (1998). Measuring Stream Shade. *Journal of the North American Benthological Society*, 17, 250-260

Davies-Colley, R.J., & Rutherford, J.C. (2005). Some approaches for measuring and modelling riparian shade. *Ecological Engineering*, 24, 525-530

Davies-Colley, R.J., Meleason, M.A., Hall, R.M.J., & Rutherford, J.C. (2009). Modelling the time course of shade, temperature, and wood recovery in streams with riparian forest restoration. *New Zealand Journal of Marine and Freshwater Research, 43*, 673-688

Detenbeck, N. E., A. C. Morrison, R. W. Abele, and D. A. Kopp (2016), Spatial statistical network models for stream and river temperature in New England, USA, *Water Resour. Res.*, 52, 6018–6040

DeWalle, D.R. (2008). Guidelines for Riparian Vegetative Shade Restoration Based Upon a Theoretical Shaded-Stream Model1. *JAWRA Journal of the American Water Resources Association*, 44, 1373-1387

DeWalle, D.R. (2010). Modeling Stream Shade: Riparian Buffer Height and Density as Important as Buffer Width1. *JAWRA Journal of the American Water Resources Association*, 46, 323-333

Dietrich, J.T. (2016). Riverscape mapping with helicopter-based Structure-from-Motion photogrammetry. *Geomorphology, 252*, 144-157

Dietrich, J.T. (2017). Bathymetric Structure-from-Motion: extracting shallow stream bathymetry from multi-view stereo photogrammetry. *Earth Surface Processes and Landforms, 42*, 355-364

Dugdale, S.J., Hannah, D.M., & Malcolm, I.A. (2017). River temperature modelling: A review of process-based approaches and future directions. *Earth-Science Reviews, 175*, 97-113

Dugdale, S.J., Malcolm, I.A., Kantola, K., & Hannah, D.M. (2018). Stream temperature under contrasting riparian forest cover: Understanding thermal dynamics and heat exchange processes. *Science of The Total Environment, 610–611*, 1375-1389

Elliott, J.M., & Elliott, J.A. (2010). Temperature requirements of Atlantic salmon Salmo salar, brown trout Salmo trutta and Arctic charr Salvelinus alpinus: predicting the effects of climate change. *Journal of Fish Biology, 77*, 1793-1817

Fabris, L., Malcolm, I.A., Buddendorf, W.B., & Soulsby, C. (2018). Integrating process-based flow and temperature models to assess riparian forests and temperature amelioration in salmon streams. *Hydrological Processes*, DOI: 10.1002/hyp.11454

Fonstad, M.A., Dietrich, J.T., Courville, B.C., Jensen, J.L., & Carbonneau, P.E. (2013). Topographic structure from motion: a new development in photogrammetric measurement. *Earth Surface Processes and Landforms, 38*, 421-430

Garner, G., Hannah, D.M., & Watts, G. (2017a). Climate change and water in the UK: Recent scientific evidence for past and future change. *Progress in Physical Geography, 41*, 154-170

Garner, G., Malcolm, I.A., Sadler, J.P., & Hannah, D.M. (2014). What causes cooling water temperature gradients in a forested stream reach? *Hydrology and Earth System Sciences, 18*, 5361-5376

Garner, G., Malcolm, I.A., Sadler, J.P., & Hannah, D.M. (2017b). The role of riparian vegetation density, channel orientation and water velocity in determining river temperature dynamics. *Journal of Hydrology, 553,* 471-485

Getmapping (2014). *GetMapping 2m resolution Digital Surface Model (DSM) for Scotland and Wales*. Swindon: NERC Earth Observation Data Centre. Available from http://cataloque.ceda.uk/uuid/4b0ed418e30819e4448dc89a27dc8388

Ghermandi, A., Vandenberghe, V., Benedetti, L., Bauwens, W., & Vanrolleghem, P.A. (2009). Model-based assessment of shading effect by riparian vegetation on river water quality. *Ecological Engineering*, 35, 92-104

Gomi, T., Moore, R.D., & Dhakal, A.S. (2006). Headwater stream temperature response to clear-cut harvesting with different riparian treatments, coastal British Columbia, Canada. *Water Resources Research*, 42

Guenther, S.M., Gomi, T., & Moore, R.D. (2014). Stream and bed temperature variability in a coastal headwater catchment: influences of surface-subsurface interactions and partial-retention forest harvesting. *Hydrological Processes*, 28, 1238-1249

Guenther, S.M., Moore, R.D., & Gomi, T. (2012). Riparian microclimate and evaporation from a coastal headwater stream, and their response to partial-retention forest harvesting. *Agricultural and Forest Meteorology*, 164, 1-9

Guillozet, K. (2015). Shade Trading: An Emerging Riparian Forest-Based Payment for Ecosystem Services Market in Oregon, USA. *Environmental Management, 56*, 957-970

Guzy, M., Richardson, K., & Lambrinos, J.G. (2015). A tool for assisting municipalities in developing riparian shade inventories. *Urban Forestry & Urban Greening*, 14, 345-353

Hannah, D.M., & Garner, G. (2015). River water temperature in the United Kingdom: Changes over the 20th century and possible changes over the 21st century. *Progress in Physical Geography, 39*, 68-92

Hannah, D.M., Malcolm, I.A., Soulsby, C., & Youngson, A.F. (2004). Heat exchanges and temperatures within a salmon spawning stream in the Cairngorms, Scotland: seasonal and sub-seasonal dynamics. *River Research and Applications*, 20, 635-652

Hannah, D.M., Malcolm, I.A., Soulsby, C., & Youngson, A.F. (2008). A comparison of forest and moorland stream microclimate, heat exchanges and thermal dynamics. *Hydrological Processes, 22*, 919-940

Hardenbicker, P., Viergutz, C., Becker, A., Kirchesch, V., Nilson, E., & Fischer, H. (2017). Water temperature increases in the river Rhine in response to climate change. *Regional Environmental Change, 17*, 299-308

Hedger, R.D., Sundt-Hansen, L.E., Forseth, T., Ugedal, O., Diserud, O.H., Kvambekk, Å.S., & Finstad, A.G. (2013). Predicting climate change effects on subarctic–Arctic populations of Atlantic salmon (Salmo salar). *Canadian Journal of Fisheries and Aquatic Sciences*, 70, 159-168

Holtby, L.B. (1988). Effects of Logging on Stream Temperatures in Carnation Creek British Columbia, and Associated Impacts on the Coho Salmon (Oncorhynchus kisutch). *Canadian Journal of Fisheries and Aquatic Sciences*, 45, 502-515

Imholt, C., Soulsby, C., Malcolm, I.A., & Gibbins, C.N. (2013). Influence of contrasting riparian forest cover on stream temperature dynamics in salmonid spawning and nursery streams. *Ecohydrology*, 6, 380-392

Isaak, D.J., & Rieman, B.E. (2013). Stream isotherm shifts from climate change and implications for distributions of ectothermic organisms. *Global Change Biology, 19*, 742-751

Isaak, D.J., Young, M.K., Nagel, D.E., Horan, D.L., & Groce, M.C. (2015). The cold-water climate shield: delineating refugia for preserving salmonid fishes through the 21st century. *Global Change Biology, 21*, 2540-2553

Jackson, F.L., Hannah, D.M., Fryer, R.J., Millar, C.P., & Malcolm, I.A. (2017). Development of spatial regression models for predicting summer river temperatures from landscape characteristics: Implications for land and fisheries management. *Hydrological Processes, 31*, 1225-1238

Jackson, F.L., Fryer, R.J., Hannah, D.M., Millar, C.P., & Malcolm, I.A. (2018). A spatio-temporal statistical model of maximum daily river temperatures to inform the management of Scotland's Atlantic salmon rivers under climate change. *Science of The Total Environment, 612*, 1543-1558

James, M.R., & Robson, S. (2014). Mitigating systematic error in topographic models derived from UAV and ground-based image networks. *Earth Surface Processes and Landforms, 39*, 1413-1420

Jensen, J.L.R., & Mathews, A.J. (2016). Assessment of Image-Based Point Cloud Products to Generate a Bare Earth Surface and Estimate Canopy Heights in a Woodland Ecosystem. *Remote Sensing*, 8, 50

Johnson, M.F., & Wilby, R.L. (2015). Seeing the landscape for the trees: Metrics to guide riparian shade management in river catchments. *Water Resources Research*, 51, 3754-3769

Jonsson, B., & Jonsson, N. (2009). A review of the likely effects of climate change on anadromous Atlantic salmon Salmo salar and brown trout Salmo trutta, with particular reference to water temperature and flow. *Journal of Fish Biology, 75*, 2381-2447

Justice, C., White, S.M., McCullough, D.A., Graves, D.S., & Blanchard, M.R. (2017). Can stream and riparian restoration offset climate change impacts to salmon populations? *Journal of Environmental Management, 188*, 212-227

Kalny, G., Laaha, G., Melcher, A., Trimmel, H., Weihs, P., & Rauch, H.P. (2017). The influence of riparian vegetation shading on water temperature during low flow conditions in a medium sized river. *Knowledge and Management of Aquatic Ecosystems*, 418, 5-19

Langan, S.J., Johnston, L., Donaghy, M.J., Youngson, A.F., Hay, D.W., & Soulsby, C. (2001). Variation in river water temperatures in an upland stream over a 30-year period. *Science of The Total Environment, 265*, 195-207

Larjavaara, M., & Muller-Landau, H.C. (2013). Measuring tree height: a quantitative comparison of two common field methods in a moist tropical forest. *Methods in Ecology and Evolution*, 4, 793-801

Leach, J.A., & Moore, R.D. (2010). Above-stream microclimate and stream surface energy exchanges in a wildfire-disturbed riparian zone. *Hydrological Processes, 24*, 2369-2381

Leach, J.A., & Moore, D. (2017). Insights on stream temperature processes through development of a coupled hydrologic and stream temperature model for forested coastal headwater catchments. *Hydrological Processes*, 31, 3160-3177

Leach, J.A., & Moore, R.D. (2011). Stream temperature dynamics in two hydrogeomorphically distinct reaches. *Hydrological Processes*, 25, 679-690

Leach, J.A., & Moore, R.D. (2014). Winter stream temperature in the rain-on-snow zone of the Pacific Northwest: influences of hillslope runoff and transient snow cover. *Hydrol. Earth Syst. Sci.*, 18, 819-838

LeBlanc, R.T., Brown, R.D., & FitzGibbon, J.E. (1997). Modeling the Effects of Land Use Change on the Water Temperature in Unregulated Urban Streams. *Journal of Environmental Management, 49*, 445-469

Lee, A.C., & Lucas, R.M. (2007). A LiDAR-derived canopy density model for tree stem and crown mapping in Australian forests. *Remote Sensing of Environment, 111*, 493-518

Li, G., Jackson, C.R., & Kraseski, K.A. (2012). Modeled riparian stream shading: Agreement with field measurements and sensitivity to riparian conditions. *Journal of Hydrology*, 428-429, 142-151

Lim, K., Treitz, P., Wulder, M., St-Onge, B., & Flood, M. (2003). LiDAR remote sensing of forest structure. *Progress in Physical Geography: Earth and Environment, 27*, 88-106

Lisein, J., Pierrot-Deseilligny, M., Bonnet, S., & Lejeune, P. (2013). A Photogrammetric Workflow for the Creation of a Forest Canopy Height Model from Small Unmanned Aerial System Imagery. *Forests, 4*, 922-944

Loicq, P., Moatar, F., Jullian, Y., Dugdale, S.J., & Hannah, D.M. (2018). Improving representation of riparian vegetation shading in a regional stream temperature model using LiDAR data. *Science of The Total Environment, 624*, 480-490

Loinaz, M.C., Davidsen, H.K., Butts, M., & Bauer-Gottwein, P. (2013). Integrated flow and temperature modeling at the catchment scale. *Journal of Hydrology*, 495, 238-251

Lynch, A.J., Myers, B.J.E., Chu, C., Eby, L.A., Falke, J.A., Kovach, R.P., Krabbenhoft, T.J., Kwak, T.J., Lyons, J., Paukert, C.P., & Whitney, J.E. (2016). Climate Change Effects on North American Inland Fish Populations and Assemblages. *Fisheries*, 41, 346-361

MacDonald, R.J., Boon, S., & Byrne, J.M. (2014). A process-based stream temperature modelling approach for mountain regions. *Journal of Hydrology*, 511, 920-931

Malcolm, I.A., Hannah, D.M., Donaghy, M.J., Soulsby, C., & Youngson, A.F. (2004). The influence of riparian woodland on the spatial and temporal variability of stream water temperatures in an upland salmon stream. *Hydrology and Earth System Sciences, 8*, 449-459

Malcolm, I.A., Soulsby, C., Youngson, A.F., & Hannah, D.M. (2005). Catchment-scale controls on groundwater–surface water interactions in the hyporheic zone: implications for salmon embryo survival. *River Research and Applications, 21*, 977-989

Malcolm, I.A., Soulsby, C., Hannah, D.M., Bacon, P.J., Youngson, A.F., & Tetzlaff, D. (2008). The influence of riparian woodland on stream temperatures: implications for the performance of juvenile salmonids. *Hydrological Processes*, 22, 968-979

Mathews, A., & Jensen, J. (2013). Visualizing and Quantifying Vineyard Canopy LAI Using an Unmanned Aerial Vehicle (UAV) Collected High Density Structure from Motion Point Cloud. *Remote Sensing, 5*, 2164

Messinger, M., Asner, G., & Silman, M. (2016). Rapid Assessments of Amazon Forest Structure and Biomass Using Small Unmanned Aerial Systems. *Remote Sensing, 8*, 615

Michez, A., Piégay, H., Lejeune, P., & Claessens, H. (2017). Multi-temporal monitoring of a regional riparian buffer network (>12,000 km) with LiDAR and photogrammetric point clouds. *Journal of Environmental Management*, 202, 424-436

Michez, A., Piégay, H., Lisein, J., Claessens, H., & Lejeune, P. (2016). Classification of riparian forest species and health condition using multi-temporal and hyperspatial imagery from unmanned aerial system. *Environmental Monitoring and Assessment*, 188, 146

Moir, H.J., Soulsby, C., & Youngson, A.F. (2002). Hydraulic and sedimentary controls on the availability and use of Atlantic salmon (Salmo salar) spawning habitat in the River Dee system, north-east Scotland. *Geomorphology, 45*, 291-308

Moore, R.D., Spittlehouse, D.L., & Story, A. (2005a). Riparian Microclimate and Stream Temperature Response to Forest Harvesting: A Review. *JAWRA Journal of the American Water Resources Association, 41*, 813-834

Moore, R.D., Sutherland, P., Gomi, T., & Dhakal, A. (2005b). Thermal regime of a headwater stream within a clear-cut, coastal British Columbia, Canada. *Hydrological Processes, 19*, 2591-2608

Myers, B.J.E., Lynch, A.J., Bunnell, D.B., Chu, C., Falke, J.A., Kovach, R.P., Krabbenhoft, T.J., Kwak, T.J., & Paukert, C.P. (2017). Global synthesis of the documented and projected effects of climate change on inland fishes. *Reviews in Fish Biology and Fisheries, 27*, 339-361

Null, S.E., Deas, M.L., & Lund, J.R. (2010). Flow and water temperature simulation for habitat restoration in the Shasta River, California. *River Research and Applications*, 26, 663-681

Oke, T.R. (1987). *Boundary Layer Climates*. London, UK: Routledge. 464 p

Orr, H.G., Johnson, M.F., Wilby, R.L., Hatton-Ellis, T., & Broadmeadow, S. (2015). What else do managers need to know about warming rivers? A United Kingdom perspective. *Wiley Interdisciplinary Reviews: Water, 2*, 55-64

Poesch, M.S., Chavarie, L., Chu, C., Pandit, S.N., & Tonn, W. (2016). Climate Change Impacts on Freshwater Fishes: A Canadian Perspective. *Fisheries*, 41, 385-391

Rishel, G.B., Lynch, J.A., & Corbett, E.S. (1982). Seasonal Stream Temperature Changes Following Forest Harvesting. *Journal of Environmental Quality, 11*, 112-116

Robert, A. (2003). *River Processes: An introduction to fluvial dynamics*. New York: Arnold, 214p

Roth, L., Aasen, H., Walter, A., & Liebisch, F. (2018). Extracting leaf area index using viewing geometry effects—A new perspective on high-resolution unmanned aerial system photography. *ISPRS Journal of Photogrammetry and Remote Sensing*, 141, 161-175

Roth, T.R., Westhoff, M.C., Huwald, H., Huff, J.A., Rubin, J.F., Barrenetxea, G., Vetterli, M., Parriaux, A., Selker, J.S., & Parlange, M.B. (2010). Stream Temperature Response to Three Riparian Vegetation Scenarios by Use of a Distributed Temperature Validated Model. *Environmental Science & Technology*, 44, 2072-2078

Ruiz-Navarro, A., Gillingham, P.K., & Britton, J.R. (2016). Predicting shifts in the climate space of freshwater fishes in Great Britain due to climate change. *Biological Conservation, 203*, 33-42

Rutherford, J.C., Blackett, S., Blackett, C., Saito, L., & Davies-Colley, R.J. (1997). Predicting the effects of shade on water temperature in small streams. *New Zealand Journal of Marine and Freshwater Research, 31*, 707-721

Rutherford, C.J., Meleason, M.A., & Davies-Colley, R.J. (2018b). Modelling stream shade: 2. Predicting the effects of canopy shape and changes over time. *Ecological Engineering*, 120, 487-496

Rutherford, J.C., Davies-Colley, R.J., & Meleason, M.A. (2018a). Modelling stream shade: 1. Verifying numerical simulations with measurements on simple physical models. *Ecological Engineering*, 120, 441-448

Scottish Government (2012). *LiDAR for Scotland Phase I*. Edinburgh: Scottish Government, Scottish Environmental Protection Agency (SEPA), and Scottish Water. Available from www.spatialdata.gov.scot

Sridhar, V., Sansone, A.L., LaMarche, J., Dubin, T., & Lettenmaier, D.P. (2004). Prediction of stream temperature in forested watersheds. *JAWRA Journal of the American Water Resources Association, 40*, 197-213

Sun, N., Yearsley, J., Voisin, N., & Lettenmaier, D.P. (2015). A spatially distributed model for the assessment of land use impacts on stream temperature in small urban watersheds. *Hydrological Processes, 29*, 2331-2345

Tang, L., & Shao, G. (2015). Drone remote sensing for forestry research and practices. *Journal of Forestry Research*, 26, 791-797

Tetzlaff, D., Soulsby, C., Gibbins, C., Bacon, P.J., & Youngson, A.F. (2005a). An Approach to Assessing Hydrological Influences on Feeding Opportunities of Juvenile Atlantic Salmon (Salmo salar): A Case Study of Two Contrasting years in a Small, Nursery Stream. *Hydrobiologia, 549*, 65-77

Tetzlaff, D., Soulsby, C., Youngson, A.F., Gibbins, C., Bacon, P.J., Malcolm, I.A., & Langan, S. (2005b). Variability in stream discharge and temperature: a preliminary assessment of the implications for juvenile and spawning Atlantic salmon. *Hydrol. Earth Syst. Sci., 9*, 193-208

Trimmel, H., Gangneux, C., Kalny, G., & Weihs, P. (2016). Application of the model 'Heat Source' to assess the influence of meteorological components on stream temperature and simulation accuracy under heat wave conditions. *Meteorologische Zeitschrift, 25*, 389-406

Trimmel, H., Weihs, P., Leidinger, D., Formayer, H., Kalny, G., & Melcher, A. (2018). Can riparian vegetation shade mitigate the expected rise in stream temperatures due to climate change during heat waves in a human-impacted pre-alpine river? *Hydrol. Earth Syst. Sci., 22*, 437-461

Wallace, L., Lucieer, A., Malenovský, Z., Turner, D., & Vopěnka, P. (2016). Assessment of Forest Structure Using Two UAV Techniques: A Comparison of Airborne Laser Scanning and Structure from Motion (SfM) Point Clouds. *Forests, 7*, 62

Wawrzyniak, V., Allemand, P., Bailly, S., Lejot, J., & Piégay, H. (2017). Coupling LiDAR and thermal imagery to model the effects of riparian vegetation shade and groundwater inputs on summer river temperature. *Science of The Total Environment, 592*, 616-626

Westoby, M.J., Brasington, J., Glasser, N.F., Hambrey, M.J., & Reynolds, J.M. (2012). 'Structure-from-Motion' photogrammetry: A low-cost, effective tool for geoscience applications. *Geomorphology, 179*, 300-314

White, S.M., Justice, C., Kelsey, D.A., McCullough, D.A., & Smith, T. (2017). Legacies of stream channel modification revealed using General Land Office surveys, with implications for water temperature and aquatic life. *Elementa: Science of the Anthropocene*, 5

Williams, M.S., Bechtold, W.A., & LaBau, V.J. (1994). Five Instruments for Measuring Tree Height: An Evaluation. *Southern Journal of Applied Forestry*, 18, 76-82

Woltemade, C.J., & Hawkins, T.W. (2016). Stream Temperature Impacts Because of Changes in Air Temperature, Land Cover and Stream Discharge: Navarro River Watershed, California, USA. *River Research and Applications*, *32*, 2020-2031

Woodget, A.S., & Austrums, R. (2017). Subaerial gravel size measurement using topographic data derived from a UAV-SfM approach. *Earth Surface Processes and Landforms, 42*, 1434-1443

Yearsley, J.R. (2009). A semi-Lagrangian water temperature model for advection-dominated river systems. *Water Resources Research*, 45, W12405